Evaluation of Erosion Wear of slurry pump Materials

A Dissertation Submitted
In Partial Fulfillment of the Requirements
for the Degree of

Master of Engineering

in

CAD/CAM & ROBOTICS ENGINEERING

by

Jaspreet Singh

(821181002)

Under the supervision of

Mr. Satish Kumar
Assistant Professor

MECHANICAL ENGINEERING DEPARTMENT

THAPAR UNIVERSITY, PATIALA

July, 2014

CERTIFICATE

I hereby declare that the thesis entitled, **"Evaluation of Erosion Wear of slurry pump Materials"** is an authentic record of my study carried out as requirements for the award of degree of **Master of Engineering** in **CAD/CAM & Robotics Engineering at Thapar University, Patiala** under the supervision **Mr. Satish Kumar,** Assistant Professor, Mechanical Engineering Department, Thapar University, Patiala during July, 2011 to July, 2014. The matter embodied in this report has not been submitted to any other university or institute for the award of any degree.

Date: 18/07/2014

Jaspreet Singh

Jaspreet Singh

It is certified that the above statement made by the student is correct to the best of my knowledge and belief.

Mr. Satish Kumar
Assistant Professor
Mechanical Engineering Department
Thapar University Patiala-147004

Counter signed by

Dr. Ajay Batish
Professor & Head
Mechanical Engineering Department
Thapar University, Patiala

Dr. S.K. Mohapatra
Dean of Academic Affairs
Thapar University, Patiala

Acknowledgement

This thesis has been an inspiring, very challenging, but always interesting and exciting experience. In first place, I would like to express my sincere gratitude to my guide **Mr. Satish Kumar, Assistant Professor, MED, Thapar University** for acting as my thesis supervisor and giving valuable guidance, for the patience, encouragement, many fruitful discussions, and never giving up on me. Finally, I thanks to entire faculty and staff of Department of Mechanical Engineering, Thapar University, Patiala for their help, inspiration and moral support, which went a long way in successfully completion of my thesis.

Jaspreet Singh

Jaspreet Singh

Abstract

Slurry erosion is the main problem in the transportation of fly ash. Pipelines and slurry pumps are used to transport fly ash over short to medium distance through. The slurry pumps are also used for other types of slurry transportation. Due to slurry erosion slurry pump parts losses the materials. Slurry not only erodes the material but also reduces the efficiency of the slurry pump. It is necessary to reduce the effect of slurry on pump to improve the efficiency and life. So the it become necessary to reduce the slurry effect with the use of slurry resist materials for pump. Mainly coatings are used to increase the slurry resistance.

The main aim of this study is to increase the slurry resistance of the pump material. For this in this study Stainless Steel-202 grade and Grey Cast Iron is used under the effect of slurry erosion. A slurry of water and fly ash was prepared for this test. The fly ash for this purpose was collected from Guru Gobind Singh thermal plant, ropar (Punjab). To evaluate the slurry erosion Slurry Pot Tester is used. The used parameters of concentration 25 % and 45 %, speeds 800 rpm, 1100 rpm and 1400 rpm of the rotating spindle and time at 70, 120,170 and 220 minutes. To improve the performance of Grey cast iron and SS-202 coating is used. The used coating materials are $Ni+Al_2O_3$ and $Ni+Cr_2O_3$ by the thermal spraying method of HVOF. The experiment was performed on coated and uncoated of Grey Cast iron and SS-202 under the effect of different parameters. The XRD and SEM analysis was also done on the eroded and uneroded samples. Microhardness of the coated and uncoated samples was measured. After the experiment it was examined that the coated samples resisted erosion greater than the uncoated samples. It is concluded that performance of $Ni+Cr_2O_3$ coatings is better than $Ni+Al_2O_3$ coated samples.

Contents

List of Figures

List of Tables

Chapter 1

Introduction

1.1 Slurry

It is a mixture of solids and liquids, e.g. mixture of coal, fly ash, sand, and bottom ash with water. Its physical characteristics are depend upon size of particles, distribution of particles, concentration of solids in the liquid phase, size of the conduit, level of turbulence, temperature, and absolute (or dynamic) viscosity of the carrier. Slurry is a mixture of a fluid and solid particles. Generally fluid is water, in some cases air is also used such as in pneumatic conveying.

1.1.1 Types of Slurry

There are generally two types of flows:

- **Homogeneous Slurry**

A mixture of solids and liquid in which the solids are uniformly distributed. In homogeneous flows solids are uniformly distributed throughout the liquid carrier.

- **Heterogeneous Slurry**

A mixture of solids and liquid in which the solids are not uniformly distributed and tend to be more concentrated in the bottom of the pipe. Solids are not uniformly mixed in the liquid. Heavier particles tend to settle down and lighter particles tend to float. The concentration is greater towards the bottom. The heavier particles at the bottom and the lighter ones in suspension.

1.2 Pump

Pump is a device which moves the fluids (liquids or gases), or mixture of liquids and solids, by mechanical action. A pump is also used to increase the pressure energy of a fluid, used for raising fluids from a lower level to a higher level. Pump does not increase velocity of fluid but it

definite increases pressure of fluid. Fluid enters at lower pressure at inlet and fluid leaves with high pressure from outlet of pump. Pump is used for transportation of slurry, water etc.

1.3 Wear

Wear is loss of material from a component due to mechanical action from one surface with another object. Wear is one of the most common problems encountered in industrial applications. Wear reduces the life of a part. The rate of removal is generally slow, but steady and continuous. Wear depends upon material properties like hardness, strength, ductility, work hardening etc. These are very important factors for wear resistance, and like surface finishing, lubrication, load, speed, corrosion, temperature properties are also equally important for wear resistance. Wear may be occurred due to corrosion, abrasion and erosion.

1.3.1 Types of Wear

- Adhesive wear
- Abrasive wear
- Corrosive wear
- Surface fatigue wear
- Erosion wear

1.3.2 Symptoms and Appearance of Different Types of Wears

Table 1.1 Symptoms and appearance of different types of wears.

Type of wear	**Symptoms**	**Appearance of the worn out surface**
Abrasive wear	Presence of clean furrows cut out by abrasive particles	Grooves
Adhesive wear	Metal transfer is the prime symptom	Seizure, catering rough and turn out surfaces.

Erosion wear	Presence of abrasive in fast moving fluid and short abrasion furrows	Waves and Troughs
Corrosion wear	Presence of metal corrosion products	Rough pits and depression
Fatigue wear	Presence of subsurface and cracks accompanied by picks and spalls	Sharp and angular edges

1.3.3 Parameters Affecting Erosion Wear of a Material

- **Impact angle**

  Impact angle is defined as the angle between the target surface and the direction striking velocity of the solid particle. The variation of erosion wear with the impact angle depends on the characteristics of the target surface material namely brittle or ductile type.

- **Velocity of solid particles**

  It is main parameter which affects the erosion wear of a material. Velocity of solid particle strongly affects the erosion wear. Particle velocity proportional to erosion rate. Particle velocity increases the erosive wear of the surface.

- **Hardness**

  Hardness of the material affects the erosion wear of the material. Hardness can be define as the resistance to permanent deformation.Surface hardness as well as hardness of solid effects on the erosion wear mechanism. If hardness of the substrate is more than erosion wear rate reduces.

- **Particle size and shape**

  Particle size and shape is also one of the important parameter, which affect erosion wear. Solid particle size important to erosion wear. The erosion wear increases with increase in particle size.

- **Solid concentration**

  Solid concentration is the ratio of mixture of fluid and solid particles. Solid cocentration is amount of solid particles by weight or by volume in the fluid. If the concentration of particle increases more particles strike the surface of impeller which increase the erosion rate.

1.4 Erosion Wear

Erosion wear is a process of progressive removal of material from a target surface due to repeated impacts of solid particles. The particles suspended in the flow of solid liquid mixture erode the wetted passes limiting the service life of equipment used for slurry transportation system. Erosion wear caused by the kinetic energy transferred to target surface by impinging solid particles. Material loss of target material is higher for higher kinetic energy of impinging particle. So impact velocity largely affects the erosion wear of target material. Also erosion wear depends on the angle with which erodent strikes at target surface (impact angle), slurry concentration, erodent size, erodent shape etc. the extent of erosion wear changes material to material of target surface.

1.5 Material

A material is that out of which anything may be made.

1.5.1 Types of Material

- **Brittle Materials**

The material that does not allows it to be bent, drawn out (as a wire or sheet).

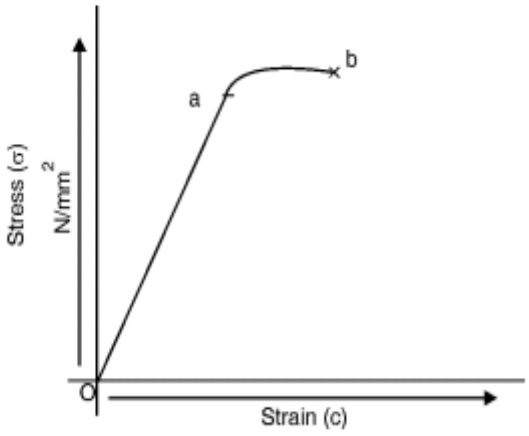

Figure 1.1 Stress – strain diagram for a brittle material

Point a is the limit of proportionality and point b is the breaking point. The curve does not have a yield point.

- **Ductile Materials**

The property of a material that allows it to be bent, drawn out (as a wire), or otherwise deformed without breaking is known as ductility. Materials that offer such property are known as ductile materials.

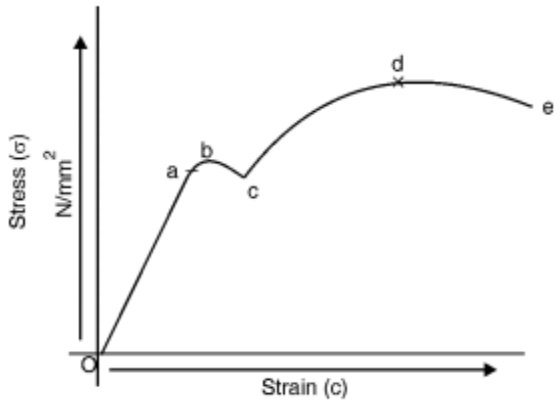

Figure 1.2 Stress – strain diagram for a ductile material

Point a: Limit of proportionality. 0-a is a straight line and stress is proportional to strain. The slope of the line gives the value of Young's Modulus of Elasticity. Point b gives the yield point of the material and is called the elastic limit. This is the greatest stress that the material can endure without taking up permanent set after load is removed. Point c is called lower yield point. Point d gives the maximum or ultimate stress. Point e is called the breaking point and material fails.

1.6 Thermal Power Plants

Thermal power plants are the modern technique to produce the electricity power with use of coal fired with rankine cycle based thermodynamics system. Mostly thermal plants used heat produced by coal fuel oil or natural gas. All thermal power plants convert heat energy into mechanical energy, and then into electricity. This is done by using heat to turn water into steam

and then directing the steam at a turbine. The steam turns the turbine blades, converting heat into mechanical power. This in turn runs the generator, which creates electricity.

1.7 Ash Transportation

Ash is the substance produced by the combustion of coal used in the thermal plants. Ash disposal in thermal power plants is a highly environmentally sensitive issue. India is currently producing in excess of 100 million tonnes of coal ash. Currently fly ash and bottom ash are mixed together and transported hydraulically to ash ponds. The end uses of fly ash and bottom ash are different as their properties are different. Mixing them during transportation would affect the end usage of both forms of ashes.

1.7.1 Ash Transportation Forms

- Dry transportation
- Wet transportation

1.7.2 Classification of Wet Disposal

- Low concentration (10% to 30%)
- Medium concentration (40% to 50%)
- High concentration (60% to 70%)

1.8 Steps for Slurry Transportation

The basic slurry transportation a system consists is:

- Slurry preparation
- Pipelines and pumps
- Terminal

In the slurry transportation, firstly the solids are converted into powder form, and stored in the storage place. Then water or the liquid is mixed to the powdered solid to make slurry and is pumped with the help of pumps. The pumped slurry is then transported to the next station using pipelines. Pipelines can transport the slurry to longer distances easily. The next station is the

dewatering station where water is removed from the slurry and the powdered form is transported for further utilization or it is sent to the dumping yard far away.

1.9 Wear Problem in Ash Transportation

Wear in transportation takes place because of two reasons corrosion and erosion. These mechanisms are different in nature. Corrosion of a metal is an electro-chemical phenomenon and in slurry pipeline it is generally due to the dissolved oxygen in the slurry. Corrosion can be controlled by passivating either the anodic or the cathodes reactions of the pipe wall. Elimination of dissolved oxygen and the adjustment of slurry pH can also reduce the corrosion rate. Erosion of metal occurs due to the dynamic action of the moving particles on the pipe wall and is generally more pronounced than corrosion in slurry pipeline systems. During the transportation of slurry erosion occurs in the slurry pipe line and pumps which are used in transport of the slurry. Slurry in both pipes and pump is the main problem. This should be reduced as possible to increase the life of equipment used in transportation. The parameters that affect erosion wear in pipelines are:

- Due to Solid particles
    - Size of particles
    - Particle hardness
    - Particle density
    - Shape and composition of particles
- Due to carrier fluid
    - Corrosive nature of fluid
    - Density and viscosity of fluid
- Effect of slurry properties
    - Effect of concentration of slurry
    - Viscosity and density of slurry
- Condition of flow
    - Laminar/ Turbulent
    - Heterogeneous/ Homogeneous
    - Velocity of flow
- Characteristics of pipe material

- Strength of pipe
- Ductility and hardness of pipe

1.10 Erosion Wear Testing Apparatus

- Miller test apparatus
- Slurry pot tester
- Jet impingement tester (JIT)
- Falling jet apparatus
- Jet in slit apparatus
- Centrifugal erosion tester
- Coriolis erosion tester

1.10.1 Slurry Pot Tester

This test rig is small in size, simple in design, easy to operate, economical and can be used to generate experimental data at an accelerated rate. In this test rig, the wear specimens are rotated in a cylindrical pot containing solid-liquid mixture. The specimen is hold in a fixture connected to a rotating steel shaft. The propeller having two blades at the end connected to a rotating shaft keeps the solid particle suspended in a liquid. The relative motion between the wear specimen and the slurry causes erosion wear. Effect of various operating parameters like concentration, velocity and impact angle can be easily calculated.

1.10.2 Jet Impingement Tester (JIT)

In this type of test rig, a flat specimen can be oriented at different impact angles in the range of 0 to 90 degree. It comprises of a pump and an ejector to issue a jet through a nozzle. Jet impingement tester simulates the wear for direct impact of solid particles in equipment such as pumps, bends, tee junctions, elbows, contractions etc. This type of tester provides very good control over various parameters of erosion wear.

1.10.3 Coriolis Erosion Tester

In this test rig, the wear specimens are to be fixed on the channels. The slurry is accelerated centrifugally from a rotating bowl through two small radial channels located at 180º apart. The Coriolis force increases the slurry interaction with the back wall of the wear specimens.

1.11 Coating

Coating is layer of one material on another material to get the desired properties of base material or to change some properties of base material. Coating is mainly applied for corrosion resistance, erosion resistance, friction resistance etc.

1.11.1 Types of Coating Methods

There are mainly four types of coating as given below:

- Physical vapor deposition coating
- Chemical vapor deposition coating
- Electroplating coating
- Thermal spray coating

- **Physical vapor deposition**

Physical vapor deposition (PVD) describes a variety of vacuum deposition methods used to deposit thin films by the condensation of a vaporized form of the desired film material onto various work piece surfaces. The coating method involves purely physical processes such as high-temperature vacuum evaporation with subsequent condensation. Virtually any coating metal can be applied by PVD and environmental concerns associated with liquid wastes can be avoided.

- **Chemical vapor deposition**

Chemical vapor deposition (CVD) is a chemical process used to produce high-purity, high performance solid materials. The process is often used in the semiconductor industry to produce thin films. In typical CVD, the wafer (substrate) is exposed to one or more volatile precursors, which react and/or decompose on the substrate surface to produce the desired deposit. Frequently, volatile by-products are also produced, which are removed by gas flow

through the reaction chamber. Micro fabrication processes widely use CVD to deposit materials in various forms, including: monocrystalline, polycrystalline, amorphous, and epitaxial. Typical coating thickness cover a very wide range up to 100μm depending on the specific coating applied.

- **Electroplating**

Electroplating, the process of coating a metal object with a thin layer of another metal by means of electrolysis. The electroplated coating is usually no more than .002 inch (.05 mm) thick. Electro-forming is a similar process except that the thin layer is applied to a nonmetal that is later destroyed. Electroplating is used to give metal objects a better appearance or to protect them from corrosion, wear, or rust. Tableware, trays, decorative pieces, and jewelry are plated with gold or silver to make them more attractive. Copper is coated with chromium to protect it from corrosion. Electroplating is a plating process that uses electrical current to reduce captions of a desired material from a solution and coat a conductive object with a thin layer of the material, such as a metal. Electroplating is primarily used for depositing a layer of material for a desired property to a surface that otherwise lacks the property. The process used in electroplating is called electro deposition.

- **Thermal Spray Coating Process**

Thermal spraying techniques are coating processes in which melted (or heated) materials are sprayed onto a surface. The "feedstock" (coating precursor) is heated by electrical (plasma or arc) or chemical means (combustion flame). Thermal spraying can provide thick coatings (approx. thickness range is 20 micrometers to several mm, depending on the process and feedstock), over a large area at high deposition rate as compared to other coating processes such as electroplating, physical and chemical vapor deposition. Coating materials available for thermal spraying include metals, alloys, ceramics, plastics and composites. They are fed in powder or wire form, heated to a molten or semi molten state and accelerated towards substrates in the form of micrometer-size particles. Combustion or electrical arc discharge is usually used as the source of energy for thermal spraying. Resulting coatings are made by the accumulation of numerous sprayed particles. The surface may not heat up significantly, allowing the coating of flammable substances. Coating quality is usually assessed by measuring

its porosity, oxide content, macro and micro-hardness, bond strength and surface roughness. Generally, the coating quality increases with increasing particle velocities.

1.11.2 Types of Thermal Spray Coatings

- Plasma spraying
- Detonation spraying
- Wire arc spraying
- Flame spraying
- High velocity oxy-fuel coating spraying (HVOF)
- Warm spraying
- Cold spraying

1.12 High Velocity Oxy-Fuel Coating Spraying (HVOF)

A class of thermal spray processes called high velocity oxy-fuel spraying. A mixture of gaseous or liquid fuel and oxygen is fed into a combustion chamber, where they are ignited and combusted continuously. The resultant hot gas at a pressure close to 1 MPa emanates through a converging–diverging nozzle and travels through a straight section. The fuels can be gases (hydrogen, methane, propane, propylene, acetylene, natural gas, etc.) or liquids (kerosene, etc.). The jet velocity at the exit of the barrel (>1000 m/s) exceeds the speed of sound. A powder feed stock is injected into the gas stream, which accelerates the powder up to 800 m/s. The stream of hot gas and powder is directed towards the surface to be coated. The powder partially melts in the stream, and deposits upon the substrate. The resulting coating has low porosity and high bond strength. HVOF coatings may be as thick as 12 mm (1/2"). It is typically used to deposit wear and corrosion resistant coatings on materials, such as ceramic and metallic layers.

Chapter 2

Literature Review

Slurry erosion wear is main problem to transport a slurry from one station to another station, in India most of the thermal power plants use lignite coal that contains large amount of bottom ash, fly ash and other particles so there is essential to transport the slurry. From plant to the pond which is at too distance from the plant, to transport pipe lines and pumps are used to transport the slurry. Erosion wear may be occurred the pipe lines and in pumps. On the basis of this author is motivated for the study of the erosion wear problems in the pipelines.

Zhao et al. (1999) have studied the comparison of SUS 329J1 dual phase stainless steel, in the jet-in-slit and the rotating specimen testers abrasive properties of a series of ceramic coatings with different low pressure plasma spray (LPPS) and combined LPPS/APPS (atmospheric pressure plasma spray). The erosive environments were selected as silica sand slurry and fly ash(x%)+gypsum(y%) slurries, respectively. The test results from the two testers did not always coincide although they did in general. In addition, the impact frequency, velocity and angle of particles on the surfaces of the specimens were measured and calculated, and they were used to explain the wear properties of ceramic coatings. Generally, ceramic coatings, such as Cr_2O_3 and Al_2O_3, have much improved wear resistance. But the advantages of their wear properties are decreased with increasing impingement angle. In the fly ash(x%)+gypsum(y%) slurry environments which are usually existed in the desulphurizers of thermal power plants, the most deleterious environment for the pumps is pure fly ash (fly ash(100%)+gypsum(0%) slurry.

T. Kumar et al. (2004) have studied salt bath nitrocarburizing and oxidizing of 304, 316, 304L and 316L were experimented. The experiment carried out for time period of 120, 150 and 180 minutes at a temperature of 560 ^{0} C. and oxidation process at 373^0 C for 60 minutes. Test was carried out for the above-mentioned stainless steels before and after diffusion hardening by Vickers' micro hardness and salt spray. It was found that salt bath nitrocarburizing effectively increases the hardness of stainless steels 304, 316 304L and 316L. From the microstructure of the nitrocarburized and oxidized specimens, the case depth was measured. The depth of diffusion

layer could be attributed to the attraction between the alloying elements Molybdenum and Nitrogen. Also the corrosion resistance of nitrocarburized and oxidized steels is observed to be superior to the untreated specimens.

Machiona et al. (2005) have studied the behavior of stainless steel (420, 316 grades). Experiment was performed on slurry pot erosion tester. They compared their resistance to abrasion and slurry erosion under identical conditions and the substrates thermal spray coatings based on tungsten carbide which is used in wear applications. The coatings have been deposited on stainless steel substrates using a high pressure high velocity oxy-fuel (HVOF). The tests have now been repeated with optimized WC–VC–Co powders. The present results show that the WC–VC–Co coatings produced with the optimized powders exhibit higher abrasion resistance then commercial WC–Co coatings. Replacement by VC of part of the WC hard phase in WC–Co thermal spray coatings leads to a better abrasion resistance both in dry and wet conditions because VC appears to hinder the growth of WC grains, increase the corrosion resistance of the coatings and reduce the volume fraction of cobalt through the formation of (V, W) phase which has lower density than WC. The performance of the new coatings in slurry erosion is not superior to that of conventional ones, but VC can safely partly replace WC also under slurry erosion conditions.

DSouza et al. (2005) have studied stainless steels 327, 316 as a reference and the performance of these materials is presented. Tests under erosion–corrosion conditions were performed in 3.5% NaCl solution with silica sand concentrations of 200, 500 and 1000 mg/l, at two temperatures (20 and 50 ◦C) and using an impingement velocity of 17 m/s. The material degradation caused by the interaction between corrosion and erosion on the overall material loss in erosion–corrosion environments. They was evaluate the material loss without WC Co Cr thermal spray coating by high velocity oxy-fuel (HVOF). The mechanical and electrochemical components, which contribute to degradation are isolated and evaluated using an experimental protocol comprising electrochemical techniques and scanning electron microscopy (SEM). The results show that corrosion and corrosion–erosion interactions play an important role in the overall material degradation of the HVOF coating and that the dominance of each process is critically dependent

on the environment. WC Co Cr thermal sprayed coatings can provide good protection against wear and corrosion in liquid–solid impingement when compared with stainless steels. The extent of the benefits offered by WC Co Cr is dependent on environment severity.

Srestha et al. (2005) have studied the carbon steel (BS970 EN8) and Stainless steel (UNS S31603) substrates under the effect of slurry erosion. The erosion–corrosion characteristics were carried out under the influence of a high-velocity single-phase artificial seawater jet (without solids), impinging perpendicularly onto the coating surface at 72 ms^{-1} flow velocity. Tests were performed at both 18 and 50 ^{0} C to assess the situation corrosion performance. The erosion–corrosion characteristics of Ni–Cr–Mo–Si–B coatings deposited onto carbon steel (BS970 EN8) and Stainless steel (UNS S31603) substrates with high-velocity oxy-fuel (HVOF) thermal spray process. The coatings were studied in as-sprayed, vacuum-sealed and vacuum furnace fused conditions. They had compared of the HVOF coatings were made with an uncoated stainless steel and carbon steel. Using static seawater results as a reference, the effects of the impinging flow on both the electrochemical response and the damage mechanisms were performed. The application of cathodic protection (CP) reduced the extent of deterioration. Cathodic protection can significantly reduce the material loss from HVOF sprayed Ni–Cr–Mo–Si–B coatings and from a wrought UNS S31603 under such corrosive high velocity liquid jet impingement conditions. The study showed the effect of sealing by polymer impregnation did not significantly alter the erosion–corrosion behaviour of the sprayed coating. Vacuum sealing of an HVOF sprayed Ni–Cr–Mo–Si–B coating has a very little effect in improving its overall material loss mechanism under a high-velocity liquid jet impingement condition.

Sugiyama et al. (2005) have studied slurry wear tests were carried out for base metal SCS6 and the slurry jet test apparatus was used for the slurry wear test. The flow velocity was 10–40 m/s, and the impingement angle ranged from 90◦ to 15◦.HP/HVOF thermal-sprayed arc-sprayed WC/Ni/Cr and spray fused coating of self-fluxing alloy material 41WC/Ni/Cr/Co. The slurry jet test apparatus was used for the slurry wear test. The flow velocity was 10–40 m/s, and the impingement angle ranged from 90◦ to 15◦. It was found that the volume loss rate of all test materials at 40 m/s is almost constant irrespective of impingement angle between 90◦ and 60◦, and decreases with a decreased angle. Coating hardness influences the slurry wear resistance of

the thermal sprayed materials. Cavitation erosion tests were carried out on above-mentioned materials and on HP/HVOF thermal-sprayed coatings with different compositions. The cavitation erosion resistance is not affected by material hardness, but is influenced by the density of pores in the material.

Tan et al. (2005) have studied the SS-20, 316 substrate under the effect of slurry erosion by jet impingement slurry erosion rig was used to carry out the experiment. The effects of jet velocity were investigated the solid particle erosion–corrosion performance of an experimental high velocity oxy-fuel (HVOF) sprayed Nickel–aluminum bronze (NAB). The coating consists of HVOF powders from three alloys: stainless steel alloy, nickel-based alloy and aluminum bronze alloy. This coating is used for marine applications as a cost effective replacement of existing castings and to improve component life. The coating was subjected to pure erosion, flow corrosion and erosion–corrosion tests.. By gravimetric analysis the degree of synergy was evaluated and a constant was revealed which described to what extent the presence of corrosion products/films reduces the erosivity and promotes negative synergy. Likewise, standard deviations of electrochemical current measurements are shown to reveal the presence of protective film formation under flow corrosion and film breakdown under erosion–corrosion conditions. Separation of the erosion-enhanced corrosion component revealed that at high erodent kinetic energies, erosion-enhanced corrosion dominates and generates a positive synergy. At lower energies, this coating system forms a protective film which reduces the contact conditions on impingement and a negative synergy results. Overall, correlations between the mass loss and electrochemical measurements have been established and were used to identify and quantify synergy.

Iwai et al. (2006) have studied high speed steel substrate materials under various substrate temperatures, it is proposed to use a new type of solid particle impact test (slurry jet) to swiftly evaluate wear properties of thin, single layered or multilayered coatings. By the slurry jet, 1.2 _m alumina particles were impacted at high velocity perpendicular to thin PVD coatings of TiN deposited on high speed steel substrate materials under various substrate temperatures. Since the coatings have a much higher wear resistance than the substrate material, the wear rate increases significantly to the higher level of the HSS material when the coatings are penetrated. This is

utilized in the quantification of the assessment of coating wear. A ranking of wear resistance and correlations to the coating surface hardness measured by nano-indentation tests, and coating morphology and structures are given and discussed. The TiN deposited under the highest substrate temperature proved to have the highest wear resistance although it had a relatively low hardness. The wear rate of the TiN coatings varies with the orientation of grains, that is, the *{*1 1 1*}* orientation that dominates for the high temperature deposition shows a higher wear resistance than the *{*1 0 0*}* orientation, which corresponds with the cleavage fracture behavior. Thus, it can be recommended as a screening test when evaluating coatings and coated materials.

Khameneh et al. (2006) studied mild steel substrate using jet impingement slurry tester. WC-17Co coating was deposited onto mild steel substrate using HVOF spray technique and then heat treated at different temperatures in a vacuum chamber. The coatings were then evaluated in the as sprayed and heat treated conditions. Inspections by SEM and phase analysis by XRD indicated that some brittle phases were produced at high temperature heat treatments. Generation of these phases increased the coating's hardness and decreased fracture toughness of the coating. Tribological properties were studied under dry condition by using pin on disc machine and diamond metal matrix composite disc as counter face. Wear test results showed that as sprayed deposit had the best wear resistance and its wear mechanism was sharp cutting abrasion. The weight loss in heat treated samples increased by increasing heat treatment temperature and the wear mechanisms gradually changed from cutting to gouging abrasion.

Khalid et al. (2007) have studied the wear rate of slurry pump impeller. They have designed and fabricated wear testing rig to analyse and to select parameter that can be used to determine the wear rates of slurry pump impeller. In their experiments they used an open type impeller made of cast iron with 165mm diameter and five numbers of blades. The slurry used consists of solid- liquid mixture of sand and crushed stones with water. They found out that the weight loss of the impeller is due to the material removal from the impeller as a result of erosion wear. The material is removed from several locations such as circumference, thickness of the blade, height of the blade and depth of the impeller shroud (base). Among these parameters, height loss of the blade represents the highest percentage of 60.86 percent followed by thickness loss of the blade of 35.09 percent, while the diameter loss of the impeller has the lowest loss that is 2.30 percent.

All these percentage values are related to the original values. Further they have also been concluded that the region near the center of impeller encounter less wear compared to the region at the rim of the impeller. The surface topography at the rim of the impeller showed that the materials are removed in the tangential direction to the impeller.

Oka et al (2007) have studied the effect of impacting parameters on the correlative equation was investigated for aluminium, copper, carbon steel and stainless steel specimens. They proposed a practical, predictive equation for estimating erosion damage caused by solid particle impact, which can be utilized under any impact conditions and for any type of material. The impact parameters taken into consideration were impact velocity, impact angle and size and shape of particles impacting. The material properties are mechanical properties such as material hardness. The impact angle dependence of erosion damage to these materials was also discussed. It was concluded that material hardness was an essential parameter and should be a dependent variable in terms of impact velocity dependence and impact angle dependence in the practical, predictive equations. It was also concluded that impact velocity and particle size were independent of each other, that is, particle size did not affect the impact velocity dependence of erosion damage and the impact velocity did not affect the particle diameter dependence of erosion damage.

Yildizli et al. (2007) have studied stainless steel (304), mild steel substrate under the effect of temperature. The microstructure, hardness and erosion behavior of High velocity oxy-fuel (HVOF) thermal sprayed and heat treated NiAl intermetallic coatings with three different ceria were studied through erosion tests. Test results showed that heat treatment can obviously change the erosion behavior of the HVOF thermal sprayed NiAl intermetallic coatings. After heat treatment at high temperatures, Al_2O_3 and $NiAl_2O_3$ are formed in the NiAl intermetallic coatings. Heat treated at high temperature (above 600 ◦C), the NiAl intermetallic coatings were strongly softened and exhibited higher erosion rates. Work hardening occurred during the erosion test. The degree of work hardening in thermal sprayed coating is larger than that in heat-treated coatings.

Stack et al. (2008) have studied behavior of the mild steel under the combined effects of slurry particle concentration; Slurry was used of in a synthetic sea water solution containing sand

particles and compared to the performance of mild steel exposed to similar conditions. The velocity on the erosion–corrosion of a WC/Co–Cr coating substrate was compared. The erosion and corrosion contributions and their interactions were evaluated for the materials. The results indicated that the erosion–corrosion mechanism of the coating and the mild steel showed significant differences when particle velocity and concentration were increased at various potentials. For both materials, degradation mechanisms were identified and superimposed on erosion–corrosion maps. Maps indicating levels of wastage, extent of synergy between the processes. Scanning electron microscopy was used to confirm the degradation regimes and mechanisms of material removal during the erosion–corrosion process. The effects of slurry concentration and electrochemical potential on the erosion–corrosion behavior of a WC/Co–Cr coating and a mild steel substrate have been assessed in sea water containing sand particles at various impact velocities. Mechanisms of erosion–corrosion have been identified for both the coating and the steel. Significant differences have been observed and these have been attributed to the interaction between erosion and corrosion of a monolithic material compared to a composite based coating.

Balasubramanian et al. (2008) have studied slurry wear abrasion occurs in extruders, slurry pumps, and pipes carrying slurry of minerals and ores in mineral processing industries. Abrasive slurry wear is generally defined as a mechanical interaction in which material is lost from a surface which is in contact with mixture of solid-liquid. The life of components used under slurry abrasion conditions is governed by the process parameters, properties of the abrasive particles in the slurry and the material properties. Mathematical models have been developed to estimate the abrasive slurry wear rate of carbon steel substrate and PTA hard faced stainless steel surface incorporating the main and interaction effects of abrasive particle size, slurry concentration, speed of rotation and slurry bath temperature. The abrasive particle size shows directly proportional relationship with abrasive slurry wear rate, i.e., if the abrasive particle size is large, then the abrasive slurry wear rate is higher and vice versa. The slurry concentration shows directly proportional relationship with abrasive slurry wear rate, i.e., if the slurry concentration is higher, then the abrasive slurry wear rate is higher and vice versa. The speed of rotation has inversely proportional relationship with abrasive slurry wear, i.e., if the speed of rotation increases, then the abrasive slurry wear rate decreases and vice versa. The slurry bath

temperature has very little influence on abrasive slurry wear. Of the four variables considered in this investigation, it is found that the slurry concentration has a predominant effect on wear rate of hardfaced surfaces compared to other variables. The wear resistance of PTA hardfaced stainless steel surface is four times better than carbon steel substrate surface. Microstructural analyses of the worn surfaces were carried out using SEM. Both experimental and mathematical investigations show that the wear resistance of the PTA hard faced stainless steel surface is four times better than that of the carbon steel substrate.

Desale et al. (2009) have studied the effect of particle size on erosion wear of aluminum alloy (AA 6063) has been investigated in a slurry pot tester. Eight different sized quartz particles with mean size varying between 37.5 and 655μm have been used. The wear specimens are rotated inside the pot at 3 m/s velocity with orientation angle of 30◦ and 90◦ in a sand–water mixture of 20% concentration (by weight). It was seen that the erosion wear increases with increase in mean particle size. Two distinct mechanisms are noticed for mean particle size above 200 μm and below this size for the range of parameters under this investigation. It seems that a threshold kinetic energy of impacting particle may exist, which results in change in the wear rate at a particular particle size.

Santa et al. (2009) studied the slurry and cavitation erosion resistance of six thermal spray coatings were compared to that of an uncoated martensitic stainless steel. Nickel, chromium oxide and tungsten carbide coatings were applied by oxy fuel powder (OFP) process and chromium and tungsten carbide coatings were obtained by high velocity oxy fuel (HVOF) process. The microstructure of the coatings was analyzed by scanning electron microscopy (SEM) and X-ray diffraction (XRD). The cavitation erosion resistance of the coatings was measured in a vibratory apparatus according to ASTM G32 standard and the slurry erosion tests were carried out in a modified centrifugal pump in which the samples were conveniently placed to guarantee grazing incidence conditions, as well as in a high velocity jet erosion testing machine. The results showed that the slurry erosion resistance of the steel can be improved up to 16 times by the application of the thermally sprayed coatings. On the other hand, none of the coated specimens showed better cavitation resistance than the uncoated steel in the experiments. The main mass removal mechanisms observed in all the coatings submitted to slurry erosion

were micro-cutting and micro ploughing as well as detachment of hard particles. In cavitation erosion, OFP coatings showed brittle fracture and micro cracking, and in nickel-based coatings some ductile deformation was also observed.

Tian et al. (2009) have studied erosion and corrosion problem in transportation of slurry, such as in FGD (Flue Gas Desulphurization) and chemical processing applications. Due to erosion and crrosion degradation of the pump wet-end components including pump casing, impeller and liners. The performance of a selected material is mostly dependent upon its relative corrosion and erosion resistance to the service environment. In these cases erosion, corrosion and the related synergistic effects can be very complicated since they are affected by numerous factors including solid and slurry properties, chemical contents, hydraulic conditions and temperatures. In this experimental study, sliding Coriolis erosion testing has been performed with various corrosion factors such as pH value, chlorides content and temperature to evaluate the erosion–corrosion resistance of some high-alloyed white cast irons containing different levels of chromium and other elements. Optical microscope and SEM-EDS have also been used to examine microstructure and surface conditions of tested materials. Results indicated that material loss due to corrosion factors increased as acidity-chlorides and temperature increased. At relatively high corrosion intensity, the white cast irons with higher alloy content (especially chromium) clearly showed improved corrosion resistance and combined erosion–corrosion resistance over those with lower alloy content. Under certain corrosion and hydraulic conditions, particle size is perhaps the single most influential factor on erosion–corrosion rate of the high-Cr cast iron alloys. Relatively large particles are much more effective than small ones at removing both the corroded surface layer and the fresh material, causing substantially higher rate of material loss.

Yildizli et al. (2009) have studied the erosion behaviors of the nodular and gray cast irons were studied at an intermediate and normal impact angles via an experimental setup. Erosion tests were carried out at impact angles of 30◦, 60◦ and 90◦ using angular hard particles. The particle velocity was controlled utilizing the gas pressure and was measured with rotating double discs. The results showed considerable weight loss variation as a function of the impact angles. The highest erosion rate occurred at an impact angle of 30◦ and then, two types of the cast irons

exhibited the least resistance to erosion. While the rate was at an intermediate level at 60◦, the lowest rate occurred at normal impact angle. It was found that the erosion rate of the nodular cast iron (NCI) was lower than that of the gray cast iron (GCI) at all impact angles. In all cases, the erosion appeared to have occurred by a ductile process. At oblique impact angles (30◦ and 60◦), hard erodent caused plastic flow in relatively softer surface of nodular cast iron and material removal occurred by microcutting and microploughing. During the erosive wear progress for nodular cast iron, just below the eroded surface, even though the ends of which behaved as crack nucleation agents, the deformed graphite fines were not broken off from the surface in a short time. No remarkable changes were relatively observed in the wear mechanisms. At a normal impact angle, material loss from the nodular cast iron surface occurred via gauging. Deformation spreading was also observed beneath the surface under at all impact tests. As far as gray cast iron is considered, the erodent can cause plastic yielding in the target surface and material removal went on by major ploughing with microcracking and subsurface fatigue. At a normal impact angle, the erosive wear occurred by chipping and small-scale fracture.

Ramesh et al. (2010) have studied erosion behavior of materials that consist of both brittle and ductile constituents can show erosion behavior in either a ductile or a brittle manner. High-velocity oxy-fuel thermal spraying is used with oxygen and liquid petroleum gas as the fuel gases has been used successfully to deposit WC Co/NiCrFeSiB alloy coatings on boiler tube steels. LPG fuel gas is cheap and readily available as compared to other fuels used for HVOF spraying. Under the given spray parameters, seemingly dense laminar structured coating with an average thickness of 290 micro meter and average porosity of 0.5% has been achieved. The higher cohesive strength accompanied with lower porosity of the coating deposited resulted in hardness value of 1223 HV. Substrate GrA1 steel exhibits lower steady state volume erosion rate in comparison to HVOF sprayed WC-Co/NiCrFeSIB coatings under similar test conditions. The higher hardness ratio between silica erodent particle and substrate steel might have caused the penetration of silica particles into the surface which bestow some shielding effect against impacting particles and indentation induced severe plastic deformation leads to lower erosion loss.

Chung et al. (2011) have studied the damage of materials by sand-containing water slurry erosion is enhanced as the slurry velocity increases. They used high chromium cast iron (HCCI) showed abnormal decreases in erosion of hypereutectic HCCIs having high carbon concentrations as the velocity of water–sand slurry increased from 2.5 m/s to 5 m/s. For HCCIs having lower carbon concentrations (hypoeutectic), the trend was reversed. In order to explain the abnormal erosion behavior of the hypereutectic HCCIs, microstructure, erosion–corrosion resistance, mechanical and electrochemical properties of the HCCIs under study were characterized and evaluated. It was demonstrated that the observed abnormal erosion–slurry velocity relationship was attributed to the competition between mechanical attack (erosion) and electrochemical attack (corrosion). At low slurry velocities, corrosion played an important role in erosion–corrosion, while at higher slurry velocities the mechanical attack/erosion became dominant.

Rajahram et al. (2011) have studied the effects of velocity, sand size and sand concentration on a passive metal (UNSS31603) by use a modified slurry pot erosion tester to perform in-situ electrochemical measurements during solid particle impingement to investigate. Samples are subjected to a set of erosion–corrosion experiments. The electrochemical response of UNSS31603 to the test parameters is plotted and compared to develop an understanding of the erosion–corrosion process. The current trend with variation of test parameters has been explained by an erosion enhanced corrosion synergistic effect. The current transients associated with depassivation and repassivation during solid particle impingement is observed through electrochemical noise measurements. It was observed that the increase in velocity and sand concentration increased the current levels during erosion–corrosion. However, the increase in sand size had a more complex response. Single particle impact experiments conducted revealed that the peak corrosion current and there passivation time increased with increase in velocity linear trend was seen between the peak current and the kinetic energy. A second-order exponential decay was fitted to the repassivation kinetics of the single particle impact. SEM has been used to develop a mechanistic understanding of erosion–corrosion. The surfaces cars reveal that the depth of the crater sand the length of the lips increase with increase in velocity. Micro-cracks also appear on these lips, believed to be due to corrosive action attacking the roots of these lips.

Uma et al. (2011) have studied of nickel content on the slurry erosive wear, strength and impact toughness behavior of ductile iron (PMTADI) samples subjected to a special austempering heat treatment. The nickel additions were made at five levels ranging from 0.5 to 2.5% in steps of 0.5%. Toughened ADI samples have shown an increase in slurry wear and impact toughness and a slight reduction in tensile strength than samples subjected to conventional austempering heat treatment. The results indicate that there is a significant improvement in slurry erosion resistance for 2.0% nickel PMTADI samples. Samples containing 2.0% nickel shows superior slurry erosion and impact toughness than samples containing either 1% or 2.5% nickel content. The retained austenite content, distribution of bainite and the matrix microstructure play a vital role on the slurry erosive wear and mechanical properties of PMTADI samples.

Maurer et al. (2012) have studied behavior geotextile tubes with flow of fly ash. The coal-based thermal power plants are a principal source of power generation in many industrialized countries. Fly ash and other coal combustion residuals are produced in significant quantities and must be managed, most commonly using wet-storage impoundments. Concurrent with diminishing impoundment capacity and increasing beneficial reuse of coal residuals worldwide, legislation is proposed in the US to close or liner retrofit all existing impoundments. Each of these progressions necessitates an increase in the dredging, dewatering, and transport of wet-disposal ash sludge. In recent years, geotextile tubes have increasingly been used to efficiently and economically dewater a number of low percent-solids sediments, by-products, and wastes. A laboratory investigation was conducted for studying the efficiency of geotextile tubes for dewatering hydraulically transported fly ash slurry. The dewatering behavior of unmodified fly ash was compared with that of specimens reinforced with randomly dispersed flexible PVA fibers and/or flocculated with optimized polyacrylamide. Results indicate that geotextile tubes can be effectively used for dewatering flocculated fly ash slurries and that the strength of retained fly ash can be significantly improved by adding reinforcement fibers at 1% of dry solids mass.

Grewal et al. (2013) have studied performance of mild steel and stainless steel 202 under the effect of slurry erosion and Ni–Al_2O_3 based composite coatings were evaluated under slurry erosion condition. Erosion resistance was correlated with different properties of the coatings. It

was observed that fracture toughness is an important parameter that controls the erosion resistance of coatings. Content of alumina was found to have significant influence on the erosion performance and material removal mechanism of the coatings. Erosion rates were predicted using fracture-contact model. The results were observed to lie in close proximity to the experimental results. Cracking and sapling of coating, fracture of reinforcing phase and removal of splats were observed to be the primary erosion mechanisms.

Thakur et al. (2013) have studied the slurry erosion testing was carried out using pot-type slurry erosion tester. The dry erosion testing was carried out using air-jet erosion test rig , at an impact velocity of 60m/s and 90^0 impact angle. Slurry and dry erosion behavior of HVOF sprayed WC–Co-Cr cermet coatings. The coatings were developed using the powders feed stock having WC grains in conventional and fine structured sizes. The rate of dry erosion was significantly high as compared to that of slurry erosion and it was mainly due to the particle-target impact velocities and impact angle. It was observed that reducing the size of WC grains from conventional microns to nanometers has resulted in enhanced properties of the coating. In case of slurry erosion testing, the material was removed primarily by cracking and pullout of WC grain from soft CoCr metallic binder as a result of the impacts caused by the erodent particles at a particular site and the mechanism of material removal in slurry and dry erosion was studied, discussed on microstructural investigation sand was found to be different in both the erosion conditions. The morphology of eroded surface shows crater, lip and groove formation in the binder matrix, carbide fracturing, chipping, and pull out as visible mechanism of material removal. It was observed that the cermet coating with fine WC grain exhibits higher erosion resistance as compared to conventional cermet coating due to its improved properties like micro-hardness and fracture toughness

Saarivirta et al. (2014) have studied erosive wear of four boilers steels: 16Mo3, P265GH, P91 and 304L, was examined using a four-channel centrifugal erosion tester, two types of sands and one type of ash as the erodant, the particle velocities of 10 and 20 m/s and the impact angles of 30 °, 45 ° and 90 °. The erodants varied in terms of abrasivity, which may be explained by their different composition, shape and size. Concerning the sands, abrasivity and erosivity was different with different parameters, with impacts by angular and only silicon- and oxygen-containing Sand 1 causing essentially more material losses than those by Sand 2. Furthermore,

because steady-state erosive wear was reached in the tests conducted with the sands, correlation between the extent of erosion and particle velocity could be established, enabling the deduction of the wear coefficient K. Among the studied boiler steels, wear coefficient K was the highest for the grade P265GH, suggesting the greatest efficiency of material removal by the particle impacts. When the ash was used as erodant, steady-state erosion was not reached and abrasivity and erosivity of the particles did not exhibit clear correlation.

Nguyen et al. (2014) have studied slurry erosion experiments of stainless steel stainless steel-304 were carried out using erosion tester rig, where the multiphase flows of alumina sand and water were utilized as the erodent. The results show that erosion rate was initially high and gradually reduced over the testing time. In addition, the erosion rate increased with an increase in impact velocity. The surface roughness increased with either increasing testing time or impact velocity. Further, the surface profiles of "W" shape were observed for all eroded samples.

Chapter 3

Properties of Materials and Fly Ash

3.1 Fly Ash

Fly ash is one of the major wastage materials from the combustion of coal in the thermal plant and many type of residues generated in combustion of coal in thermal power plants. Fly ash contains comprises the fine particles that rise with the flue gases. The components of fly ash vary considerably, but all fly ash includes substantial amounts of silicon dioxide (SiO2) (both amorphous and crystalline) and calcium oxide (CaO). They get collected at several locations like economizer, air preheater, mechanical dust collector, electro-static precipitators (ESP) and chimney in the thermal power plants.

3.2 Stainless Steel 202

Stainless steel grade 202 is a type of Cr-Ni-Mn stainless. The toughness of stainless steel grade 202 at low temperatures is excellent. It is one of the most widely used precipitation hardening grades, and possesses good corrosion resistance, toughness, high harness, and strength. The machinability of grade 202 stainless steel produces long, gummy chips. Machining can also be performed in the annealed condition.

3.3 Grey Cast Iron

Grey cast iron is a type of cast iron that has a graphitic microstructure. It is named after the gray color of the fracture it forms, which is due to the presence of graphite. It is the most common cast iron and the most widely used cast material based on weight. It is used for housings where tensile strength is non-critical, such as internal combustion engine cylinder blocks, pump housings, valve bodies, electrical boxes, and decorative castings.

To study the erosion wear of the materials under different parameters coatings were done on both materials of two types. The coatings were Ni+Cr_2O_3 and Ni+Al_2O_3 to increase the performance of materials. These coatings were done by the method of thermal spraying known as High Velocity Oxygen Fuel process (was discussed in 1st chapter).

3.4 Vicker's Microhardness

Hardness is a characteristic of a material, not a fundamental physical property. It is defined as the resistance to indentation, and it is determined by measuring the permanent depth of the indentation. More simply put, when using a fixed force (load) and a given indenter, the smaller the indentation, the harder the material. The Vickers hardness test method, also referred to as a microhardness test method, is mostly used for small parts, thin sections, or case depth work. The Vickers method is based on an optical measurement system. The Microhardness test procedure, specifies a range of light loads using a diamond indenter to make an indentation which is measured and converted to a hardness value. It is very useful for testing on a wide type of materials as long as test samples are carefully prepared. A square base pyramid shaped diamond is used for testing in the Vickers scale. Typically loads are very light, ranging from a few grams to one or several kilograms, although "Macro" Vickers loads can range up to 30 kg or more. The Microhardness methods are used to test on metals, ceramics, composites - almost any type of material. At Thapar University, Patiala, Micro hardness of the samples with and without coating was checked on Tester in the Material Science laboratory. Vicker's Microhardness of coated and uncoated specimen as given below.

Figure-3.1 Vicker's Microhardness

Table 3.1 Vicker's Microhardness of SS-202 and Grey cast iron of coated and uncoated specimen

S.No	Base Material	Coating	Hardness,Hv
1	SS-202	-	259
2	Grey cast iron	-	246
4	SS-202	Ni+Cr_2O_3	689
5	SS-202	Ni+Al_2O_3	610
6	Grey cast iron	Ni+Cr_2O_3	563
7	Grey cast iron	Ni+Al_2O_3	549

3.5 X-Ray Diffraction

X-Ray Diffraction (XRD) is a technique in we identify the atomic and molecular structure of a crystal. In this technique a beam of incident X-rays to diffract into many specific directions and in this a 3-D picture of density of electrons within the crystal can be produced by measuring their angles and their intensities. In this study this test was performed at Sophisticated Analytical Instrumentation Laboratory, Thapar University.

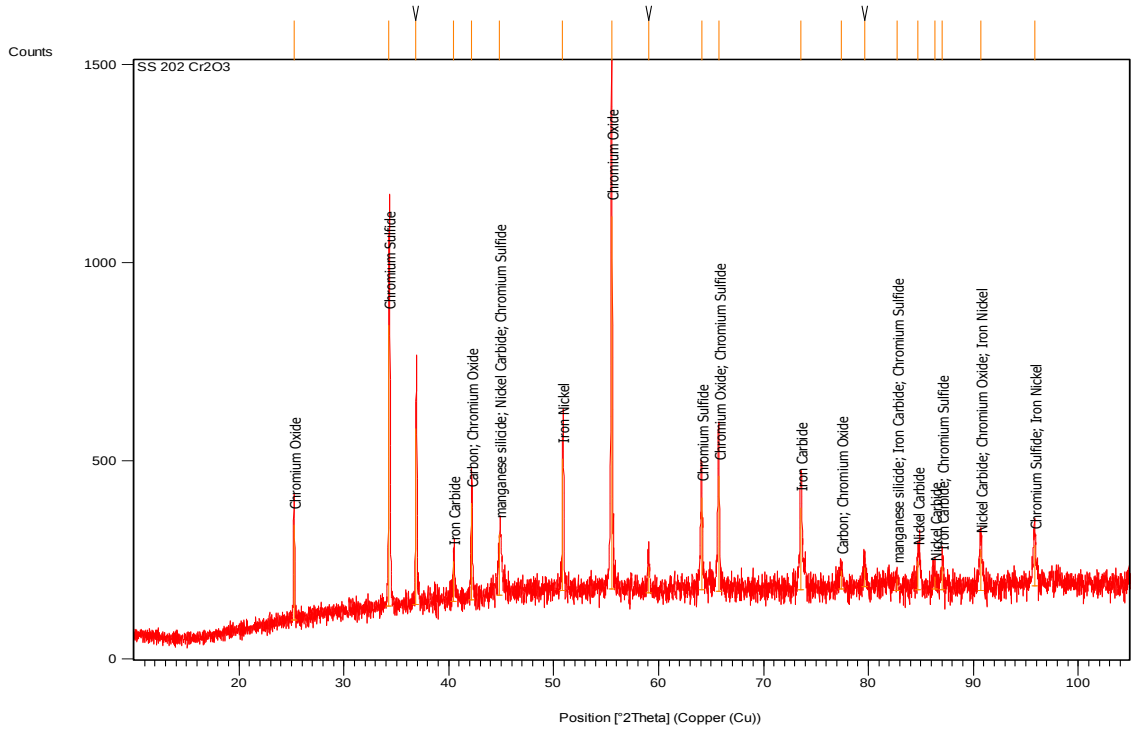

Figure-3.2 XRD graphs for mineralogical composition of Ni+Cr_2O_3 coated SS-202

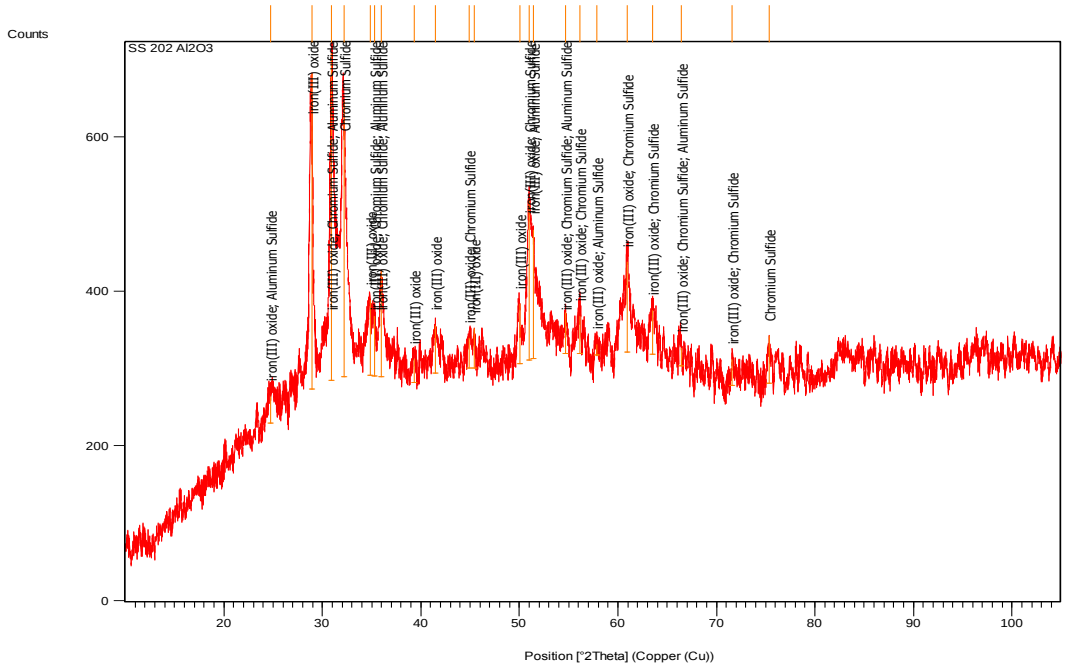

Figure-3.3 XRD graphs for mineralogical composition of $Ni+Al_2O_3$ coated SS-202

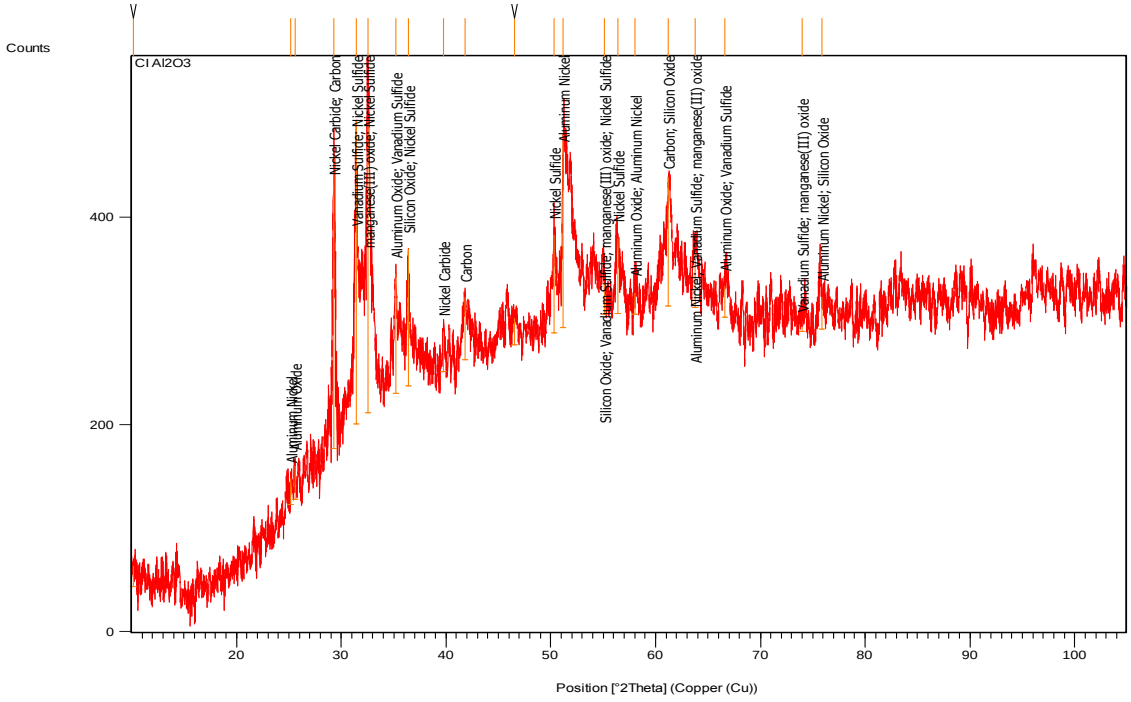

Figure-3.4 XRD graphs for mineralogical composition of $Ni+Al_2O_3$ coated Grey cast iron

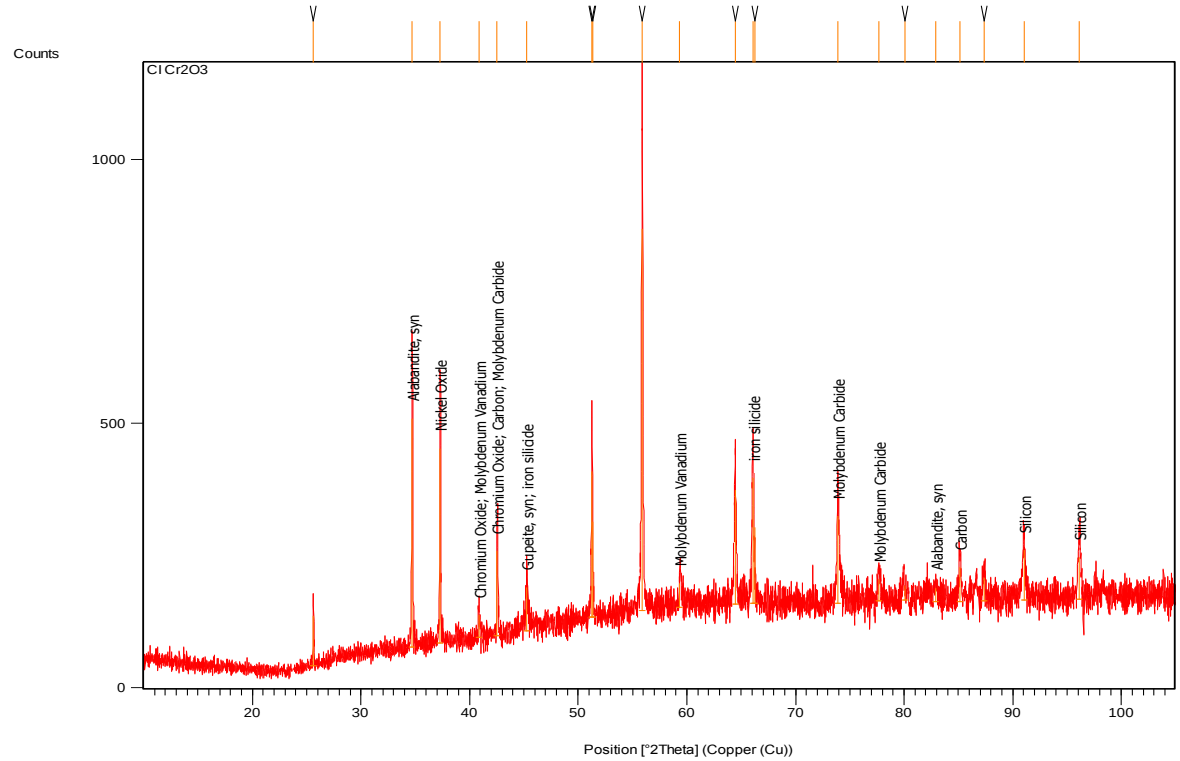

\

Figure-3.5 XRD graphs for mineralogical composition of Ni+Cr_2O_3 coated Grey cast iron

All above graphs are XRD result of the both coated specimen. From the XRD graphs it is clear that Nickel, aluminium, chromium, oxide is present of both coated materials

3.6 Scanning Electron Microscopy

A scanning electron microscope (SEM) use focused beam of electrons to produce images of sample and is a type of electron microscope. The interaction of electrons with the atoms in the sample produces various type signals and these signals can be detected and information can be collected about the sample composition and topography that is contained in it. From all given below SEM figures results the strong bonding of the coating with the specimen as we see it at X200 magnification.

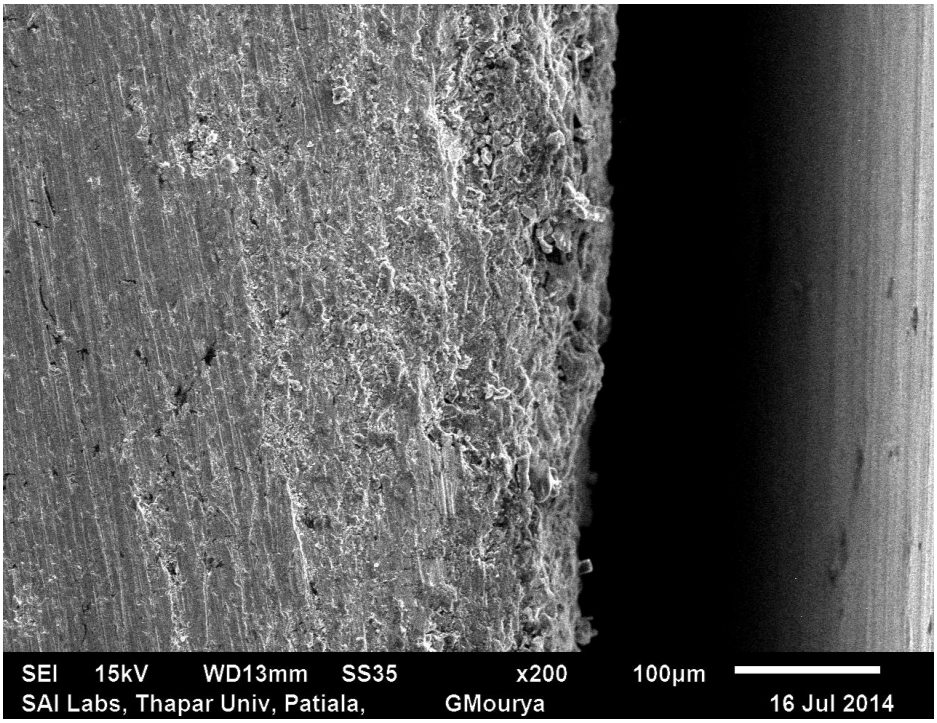

Figure 3.6 SEM analysis of Ni+Al_2O_3 coated Grey cast iron from cross-section at X200

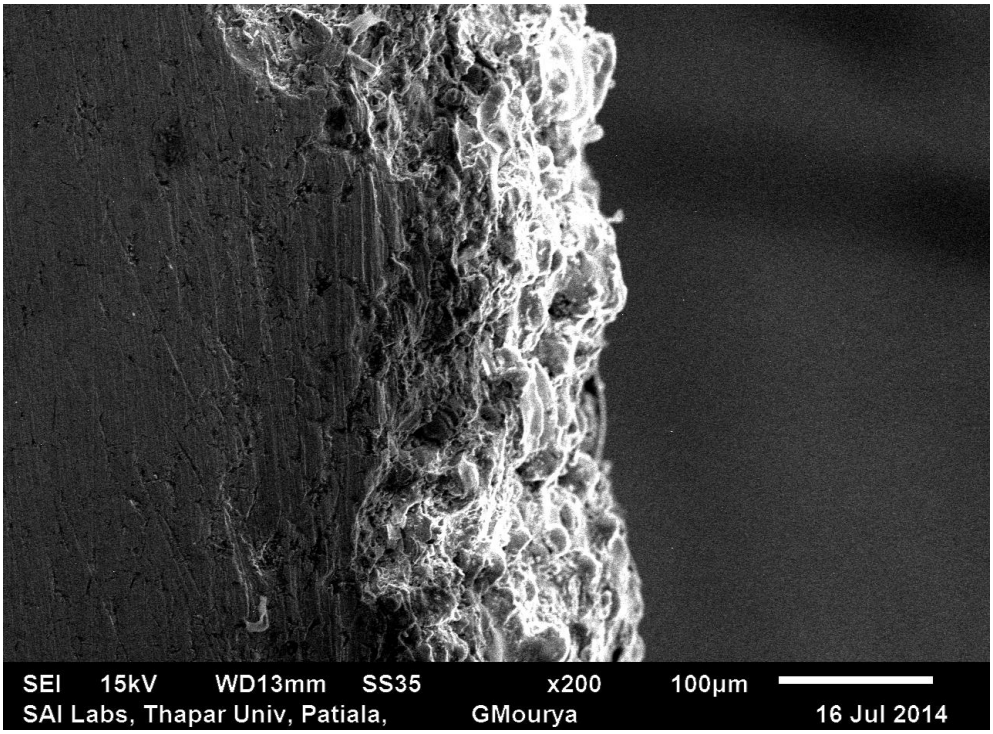

Figure 3.7 SEM analysis of Ni+Cr_2O_3 coated Grey cast iron from cross-section at X200

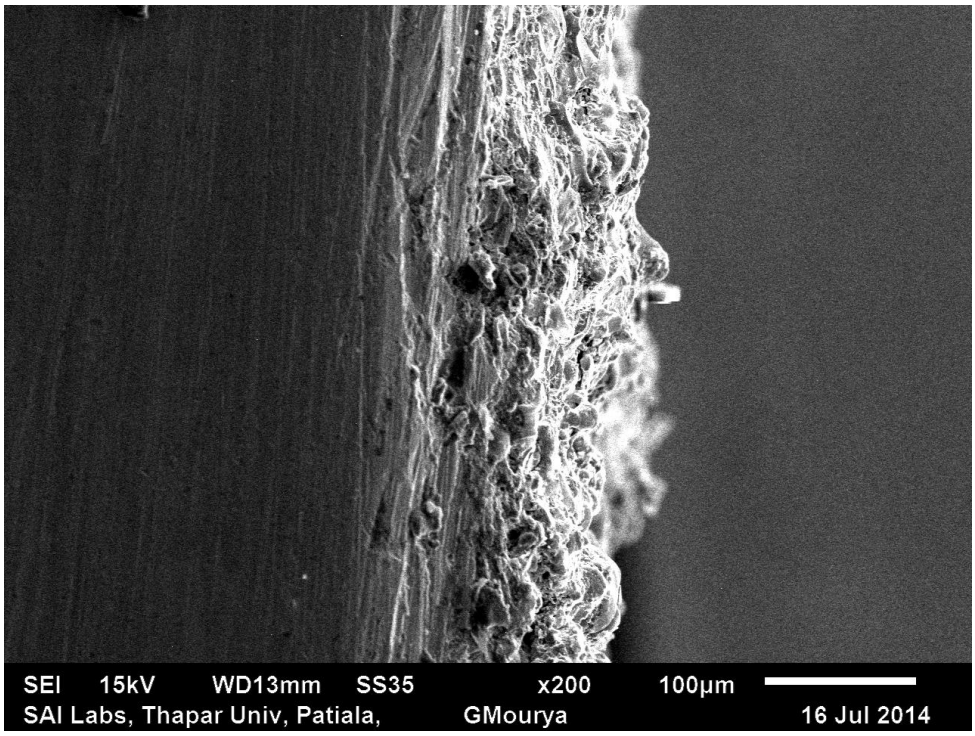

Figure 3.8 SEM analysis of Ni+Al_2O_3 coated SS-202 from cross-section at X200

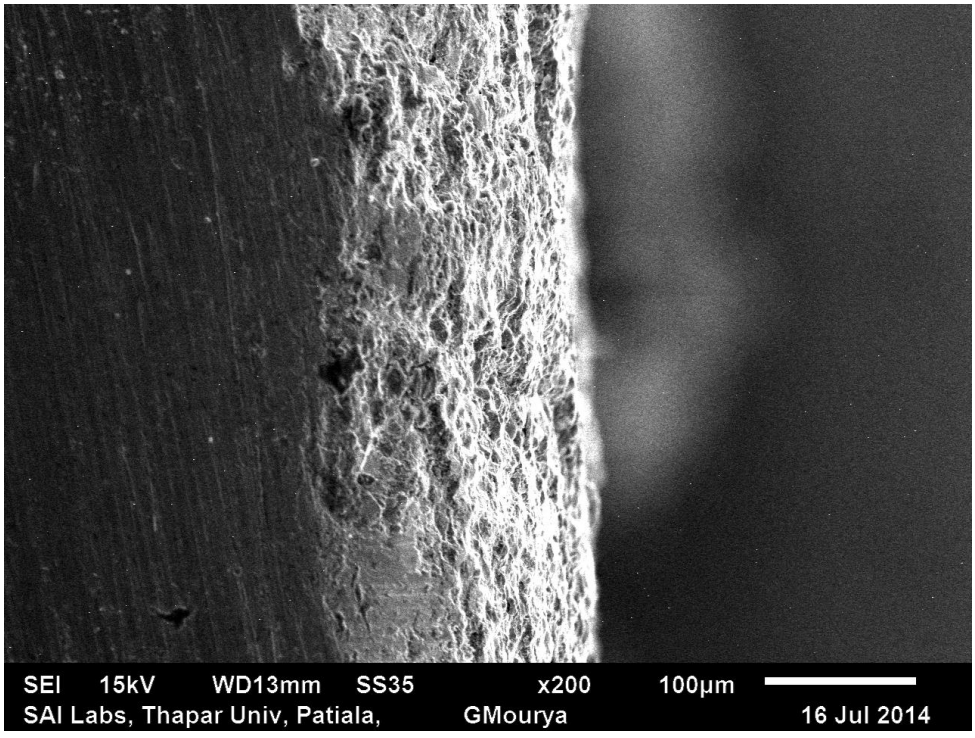

Figure 3.9 SEM analysis of Ni+Cr_2O_3 coated SS-202 from cross-section at X200

Chapter 4

Erosion Testing and Results

4.1 Slurry Pot Tester

The slurry pot tester is used in this experimental work for study of erosion of grey cast iron and stainless steel 202. The slurry pot tester TR-41 is tester to determine the erosion wear rate of the metallic materials under slurry. Erosion wear rate is determine by weighing of the metallic material before and after erosion then material loss can be measured. In another words we can say slurry pot tester TR-41 is used to determine resistance of metallic materials to mass loss under slurry. The test data produced will reproducibly rank materials in their mass loss under a specified set of conditions. The erosion wear depends on abrasive particle size, shape and hardness and the frequency of contact of specimen with the abrasives. These conditions are standardized to develop a uniform condition of wear, the tests conducted does not to duplicate all the process conditions, it should only be used to predicting the exact resistance to of a give material in a specified environment. In this experimental work slurry pot tester TR-41 is used for various test of wear erosion at different parameters.

4.1.1 Construction of Slurry Pot Tester

The slurry pot tester consists various control system and mechanical structure.

- This test rig consists of frame, base, slurry container, motor drive system, control system.
- The frame of test rig contains main part of tester. The frame is relatively rigid to avoid disturbing deformations and vibrations.
- The frame consists slurry vessel, mechanism for up and down the vessel and cooling jacket for placing slurry vessel inside it. Cooling jacket with circulating water through inlet and outlet ports. The cooling water jacket is a hollow cylinder shaped vessel made of stainless steel material.

- The water jacket is fixed with mechanical jack. Slurry vessel is made up of stainless steel material having outer dia. 120mm and height 120mm is placed inside the cooling jacket. There are fins of replaceable rubber inside slurry vessel. The specimen for test is tightened to bottom of the spindle with a stirrer to agitate slurry during spindle rotation. Slurry is mixed in correct proportion is mixed inside slurry vessel.
- The drive system consists of an Ac motor and speed can be controlled by a variable frequency drive.
- The control system controls the main operations of the test. It controls the speed (rpm) of motor and total number revolution required for the test.
- The work piece is clamped between across flat on the face of the spindle is tightened to motor shaft, below specimen a stirrer is tightened to spindle by screw to rotate along with it slurry vessel is centralized to specimen centre to immerse it completely inside slurry.
- At the above motor end cover a bush it fixed to motor shaft with a flat edge.
- In this test rig a proximity sensor is fitted which faces the flat surface bush, signal is generated when a flat surface approaches the sensor. This sensor functions in contact is less fashion and do not require any sensing mechanisms.
- In this test rig an inductive proximity sensor is used to detect the presence of wide range of metallic targets. This detection is accomplished without contacting target and its mechanically wear free.

4.1.2 Slurry Preparation

Slurry is prepared in the slurry vessel which is detachable device from testing chamber and fixed in the cooling jacket of the rig. Slurry can be prepared by mixing sand, ash and coal with water in required ratio by weight or by volume. In this experimental work fly ash is used for slurry preparation and 25 % and 45% of fly ash is used in water. Steps for preparing slurry

- Clean slurry vessel.
- Weight fly ash and water according to requirement.
- Mix ash and water properly.

Figure 4.1 External view of slurry pot tester

Figure 4.2 Internal view of slurry pot tester

Figure 4.3 View of slurry pot

4.1.3 Work Piece Dimensions

The used work piece of rectangular shape of 25mm, 75mm, 5mm. The work piece should be smooth, scratch free, machined with a central hole of diameter 8mm. In this experimental work work piece is used of grey cast iron and stainless steel 202. Following steps should be followed before using work piece for experiment.

- Clean all dirt particles from work piece.
- Work piece should be machined before use.
- Work piece should be weight before use.

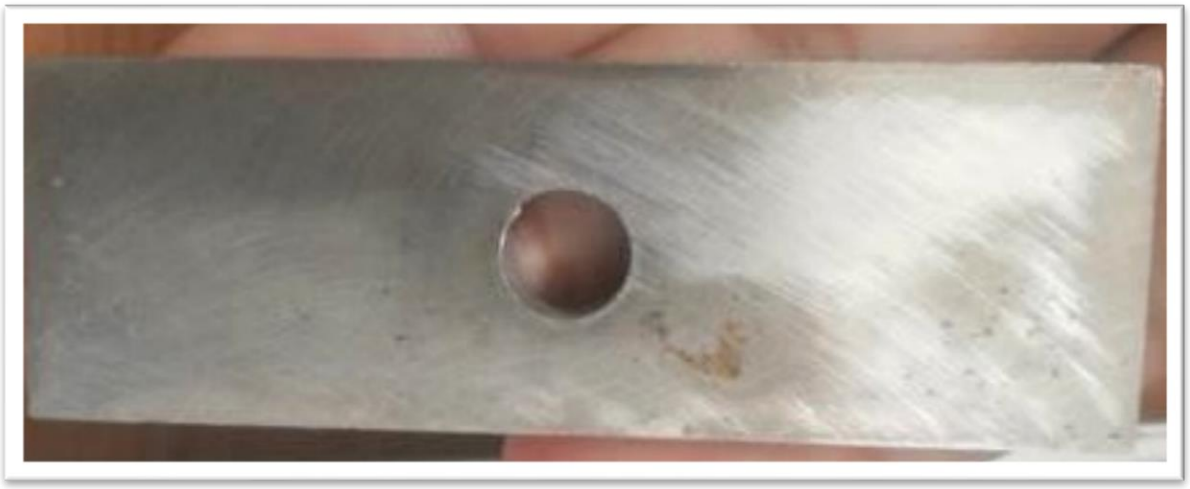

Figure 4.4 work piece sample

4.1.4 Procedure for Experiment Work

- Clean the slurry chamber to remove the remnants of slurry from the previous test.
- Weight fly ash 450gm and 250gm for different slurry concentrations and fill inside the slurry vessel.
- Fill vessel with 750gm and 550gm of water for 250gm and 450gm respectively for different concentrations.
- Weight work piece to the nearest 0.0001gm and record the value.
- Fix the work piece on the slot of spindle and tighten with stirrer.
- Connect inlet port to water source and outlet to drain.
- Switch “ON” MCB to supply power.
- Press start button on control panel and slowly rotate the SET RPM knob. In this experimental work we used the speed of 800 rpm, 1100 rpm and 1400 rpm.
- Press STOP to assets spindle rotation.
- Place the slurry vessel inside the water jacket.
- Adjust the position of water jacket to prevent leakage of the slurry.
- Set the total number of rpm for different parameters to shut off automatically after completion of time.
- Press START switch to begin work piece rotation.

- Work piece rotates in clockwise direction and the stirrer agitates slurry, the slurry rotates along the direction of rotation, the slurry rotation is arrested by vertical fins to propel it towards work piece.
- The motor will be switched OFF automatically after complete the total rpm.
- Clean the surface of each work piece.
- Allow the specimen to cool, to room temperature and remove from specimen holder
- Dry the work piece.
- Weight each work piece and calculate mass loss. And erosion wear can be calculated by taking difference of initial mass and final mass.

4.2 Parameters Used for Experiment

Following parameters were taken while performing erosion wear of slurry pump materials with or without coating.

Table 4.1: Experimental parameters and specifications

Parameters	**Specifications**
Speed	800, 1100, 1400 rpm
Concentration	25, 45 % by wt.
Time	70, 120, 170, 220 min.
Erodent used	fly ash of thermal plant
Material used	Grey cast iron and Stainless Steel 202

4.3 Results of Experiment

The erosion wear tests of coated and uncoated grey cast iron and stainless steel 202 were performed at various parameters (concentration, speed, time) with slurry of fly ash. The fly ash was collected from Guru Gobind Singh Super thermal power plant, Ropar. In this chapter we will discuss in this chapter effect of various parameters on the erosion wear of the substrate of both materials.

4.3.1 Erosion Wear Of Uncoated SS-202 At 25% And 45% Concentration

Figure 4.5 wear rate of uncoated SS-202 at 25% and 45% concentrations

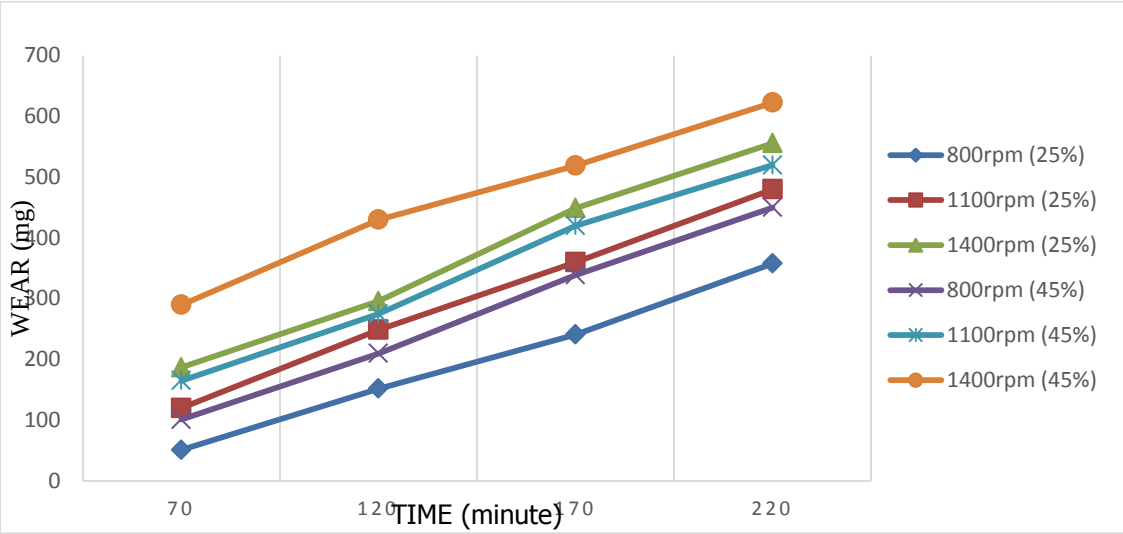

4.3.2 Erosion Wear Of Uncoated Grey Cast Iron At 25% And 45% Concentrations

Figure 4.6 wear rate of uncoated Grey Cast Iron at 25% and 45% concentrations

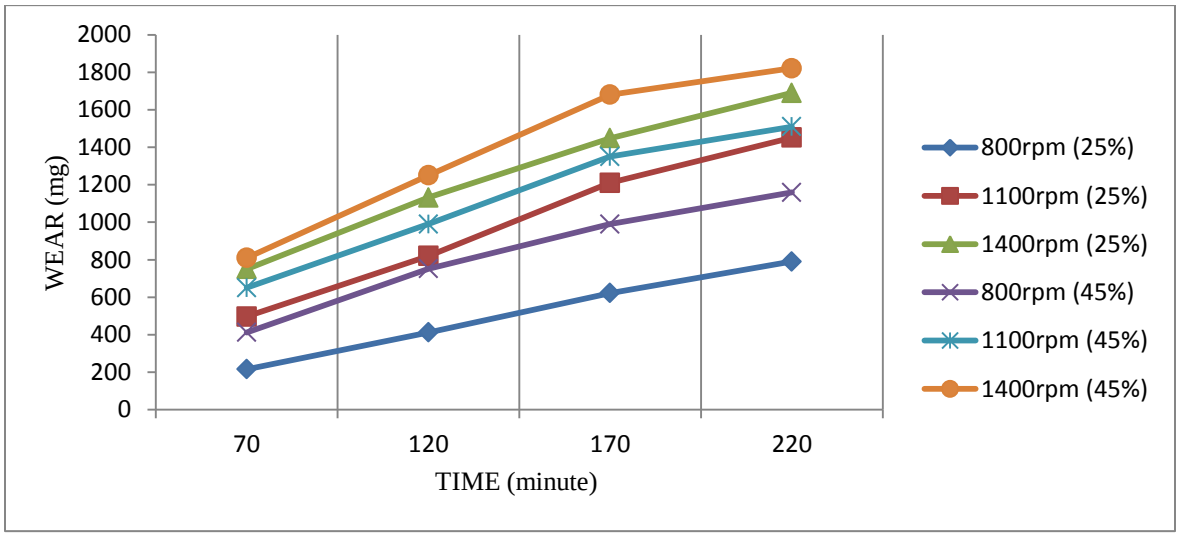

In figure 4.5 and 4.6 comparison of wear rate takes place of SS-202 and Grey Cast Iron at 25% and 45% concentrations. We can examine that from graph at same speeds the erosion wear increases with increasing the concentration of the fly ash in water and we can examine that wear depends upon speed. The wear is directly proportional to speed. The graph shows that wear of the material is minimum at lowest values of speed and concentrations i.e. 800 rpm and 25% respectively and maximum at the highest values of speed and concentrations i.e. 1400 rpm and 45% respectively.

4.3.3 Erosion Wear Of $Ni+Al_2o_3$ Coated Ss-202 At 25% And 45% Concentration

Figure 4.7 wear rate of $Ni+Al_2O_3$ coated SS-202 at 25% and 45% concentration

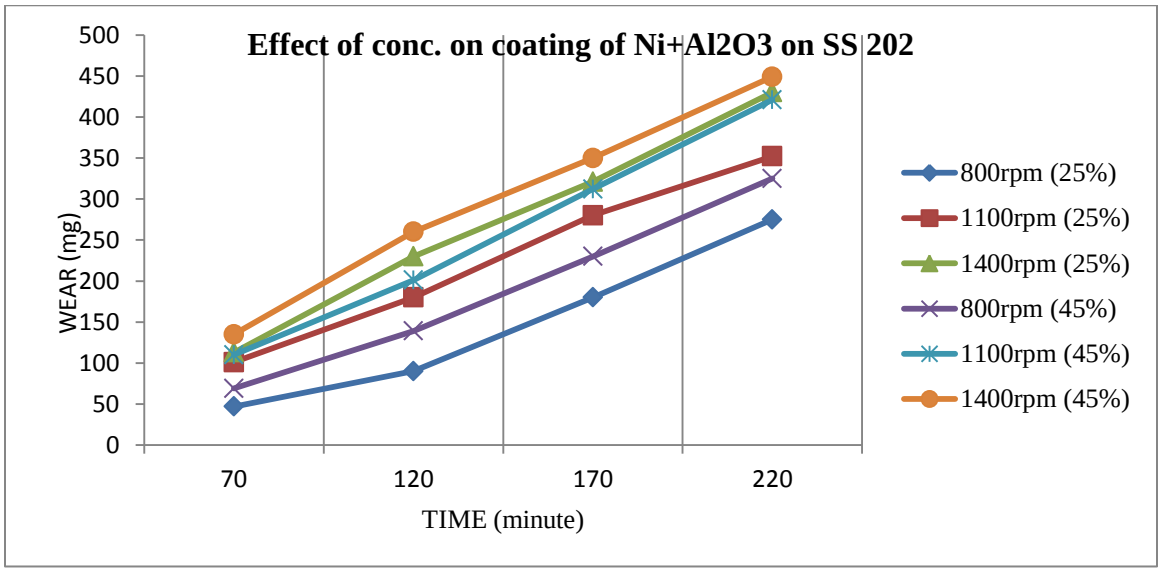

4.3.4 Erosion Wear Of $Ni+Al_2O_3$ Coated Grey Cast Iron At 25% And 45% Concentration

Figure 4.8 wear rate of $Ni+Al_2O_3$ coated Grey Cast Iron at 25% and 45% concentration

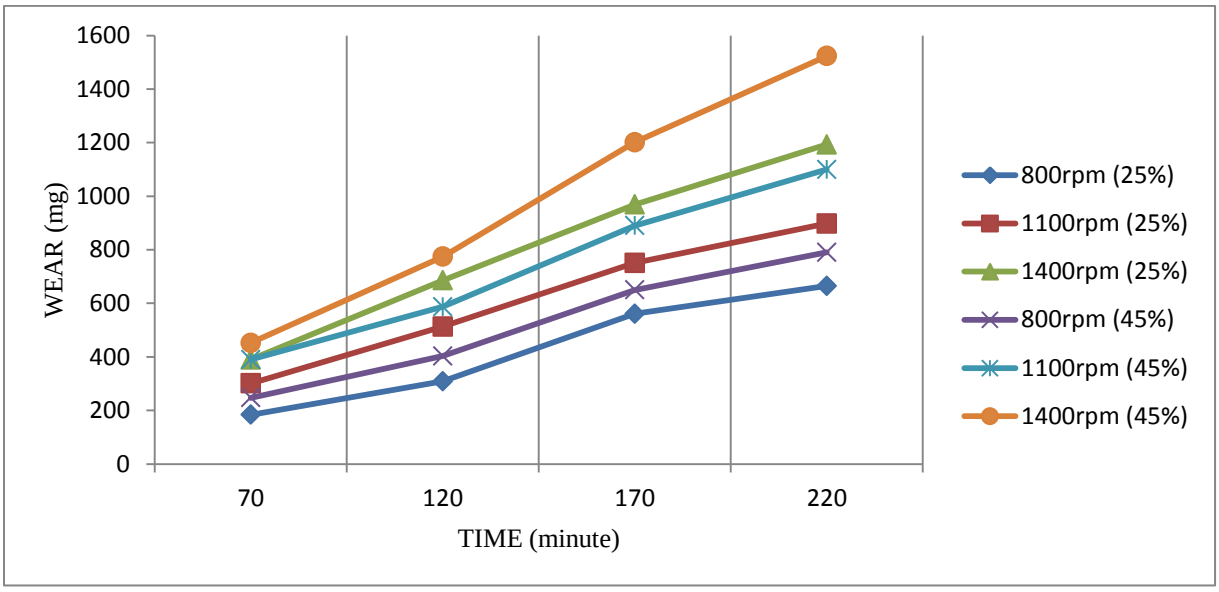

In Figure 4.7 and 4.8 in these graph comparison of wear rate of coated work piece of $Ni+Al_2O_3$ to change the desired properties of work piece. To increase the wear resistance coating of different materials is used. In comparison of uncoated and coated of same base material there is huge difference between of wear rate. In both graphs of coated and uncoated materials there is decrease in amount of wear rate. We have seen in coated graphs there is increase in wear resistance.

4.3.5 Erosion Wear Of $Ni+Cr_2O_3$ Coated SS-202 At 25% And 45% Concentration

Figure 4.9 wear rate of $Ni+Cr_2O_3$ coated SS-202 at 25% and 45% concentration

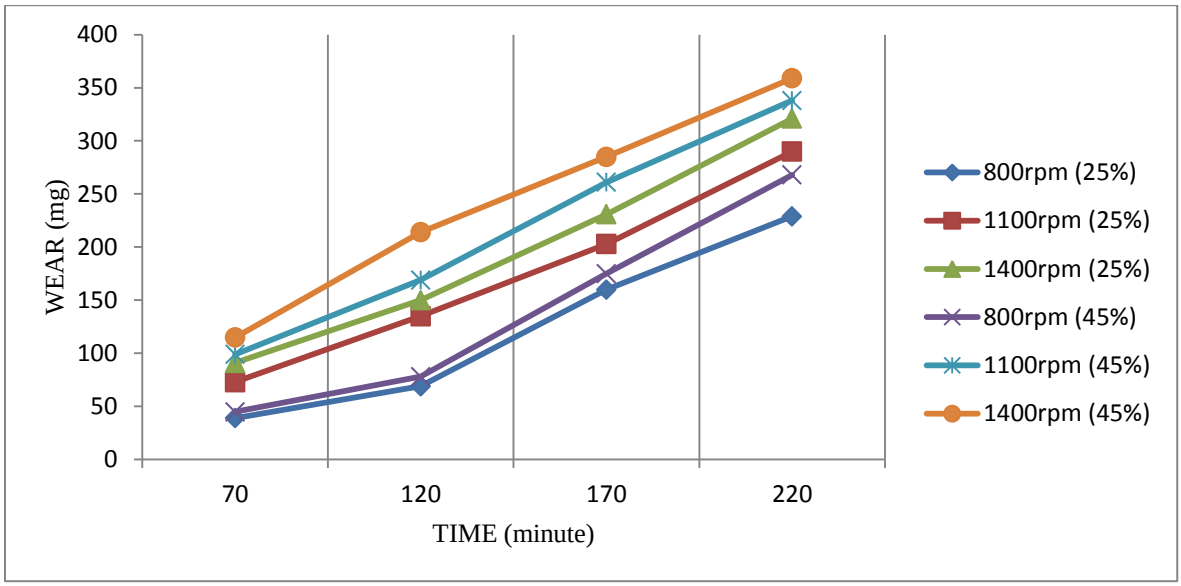

4.3.6 Erosion Wear Of $Ni+Cr_2O_3$ Coated Grey Cast Iron At 25% And 45% Concentration

Figure 4.10 wear rate of $Ni+Cr_2O_3$ coated Grey Cast Iron at 25% and 45% concentration

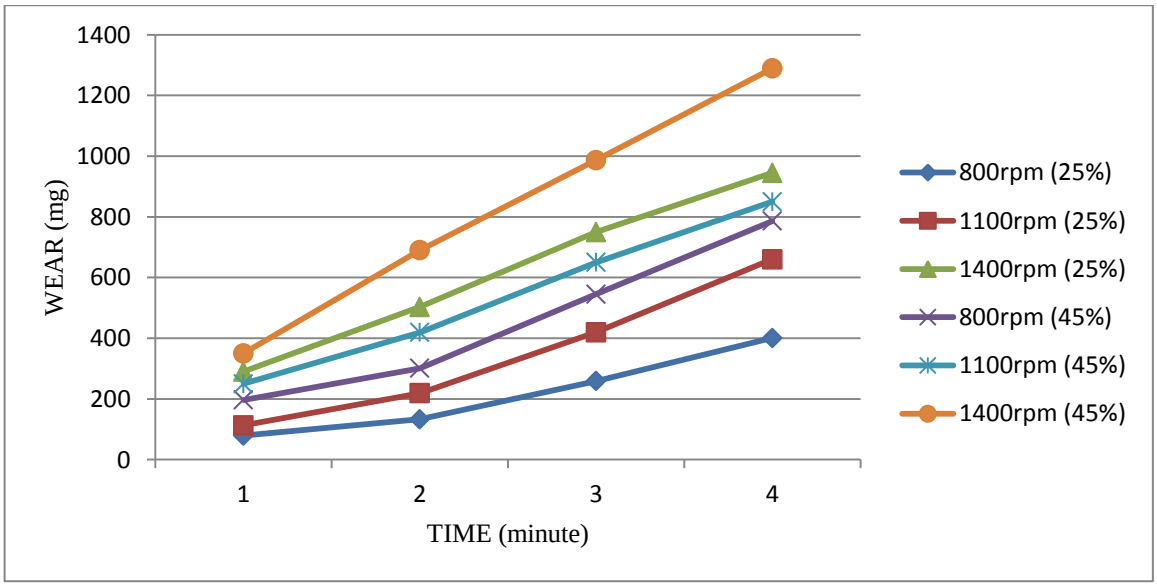

Now comparison of coating of Ni+Cr_2O_3 shows a marginal decrease in wear loss of the material. There is less material loss due to erosion wear as compare to previous coating. As we examine in the above figure 4.10 and 4.5 SS-202 of coating Ni+Cr_2O_3 shows very less wear loss in the coated state than in the uncoated state and as comparison to the Ni+Al_2O_3 based coating. But the again the trend is the same showing the increase of wear loss with concentration and speed. But it can also be noted that wear loss of Ni+Cr_2O_3coated specimens is less than Ni+Al_2O_3.

4.3.7 Comparison Of Erosion Wear Of Uncoated Grey Cast Iron, SS-202 And Ni+Al_2O_3 Coated Specimens At 25% Concentration And 800rpm

Figure 4.11 wear rate of uncoated and coating of Ni+Al_2O_3 SS-202, Grey Cast Iron at 25% concentration and 800rpm

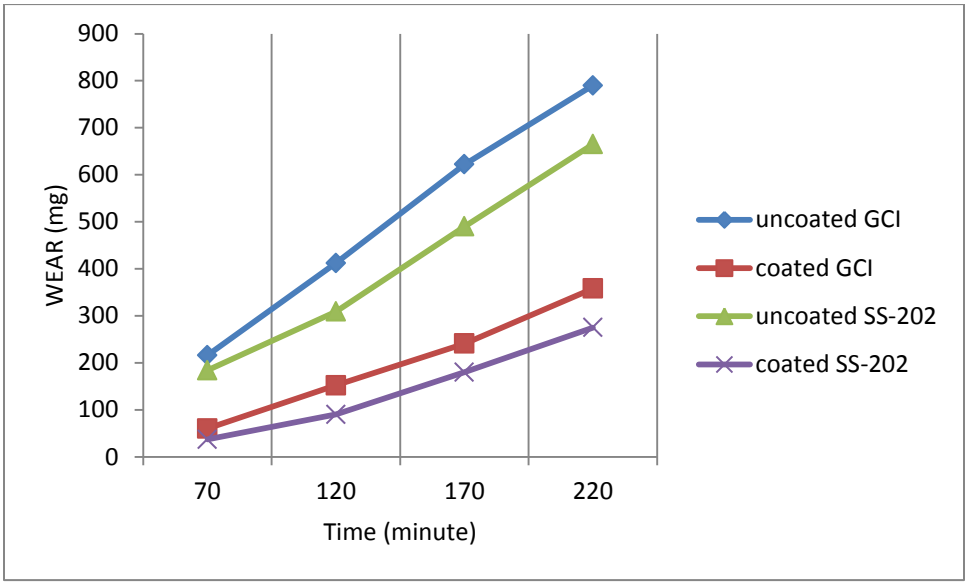

In figure 4.11 shows the comparison of uncoated and Ni+Al_2O_3 coated specimens at 800rpm and 25% concentrations. It can be seen from the above graph that the wear loss increases with the speed. This graph shows mainly to compare the wear resistance of coated materials against the uncoated materials. So it is clear from the above graph that

there is a huge difference in the material loss of a sample uncoated and the other the coated one.

4.3.8 Comparison Of Erosion Wear Of Uncoated Grey Cast Iron, SS-202 And Ni+Al_2O_3 Coated Specimens At 25% Concentration And 1100rpm

Figure 4.12 wear rate of uncoated and coating of Ni+Al_2O_3 SS-202, Grey Cast Iron at 25% concentration and 1100rpm

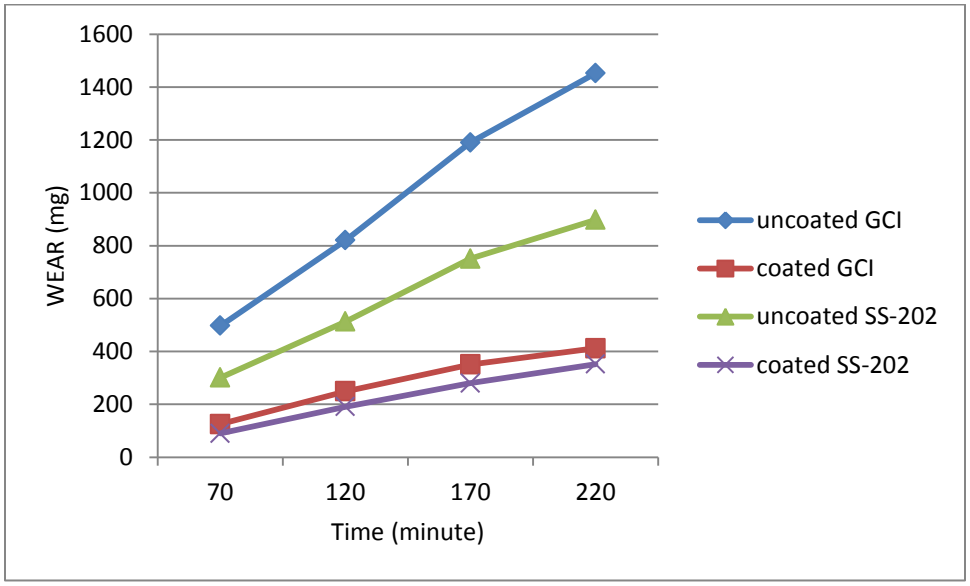

Again there is a wear difference between coated and uncoated samples. But as we compare the figures 4.11 and 4.12, it can be seen that the wear loss has increased in case of 1100rpms. Although the rate of wear is not that large but it has increased.

4.3.9 Comparison of Erosion Wear of Uncoated Grey Cast Iron, SS-202 and Ni+Al_2O_3 Coated Specimens At 25% Concentration and 1400rpm.

Figure 4.13 wear rate of uncoated and coating of $Ni+Al_2O_3$ SS-202, Grey Cast Iron at 25% concentration and 1400rpm

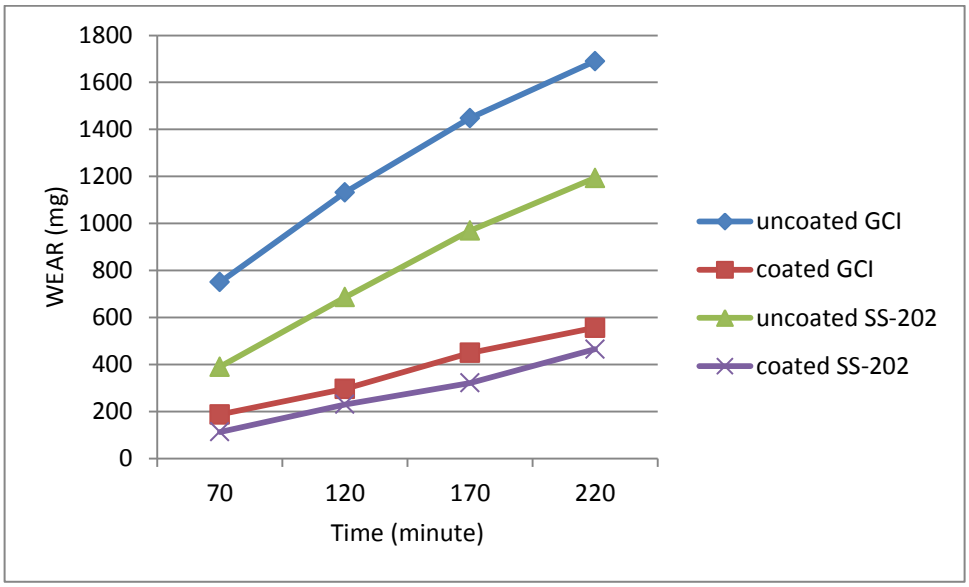

In the figures 4.11, 4.12 and 4.13 shows that wear loss increases with increase of speed of work piece. It is highest at 1400rm and lowest at 800rpm it is clear that wear is proportional to the speed of work piece. It is clear that the wear loss increases with speed.

4.3.10 Comparison of Erosion Wear of Uncoated Grey Cast Iron, SS-202 and $Ni+Cr_2O_3$ Coated Specimens At 25% Concentration and 800rpm.

Figure 4.14 wear rate of uncoated and coating of $Ni+Cr_2O_3$ SS-202, Grey Cast Iron at 25% concentration and 800rpm

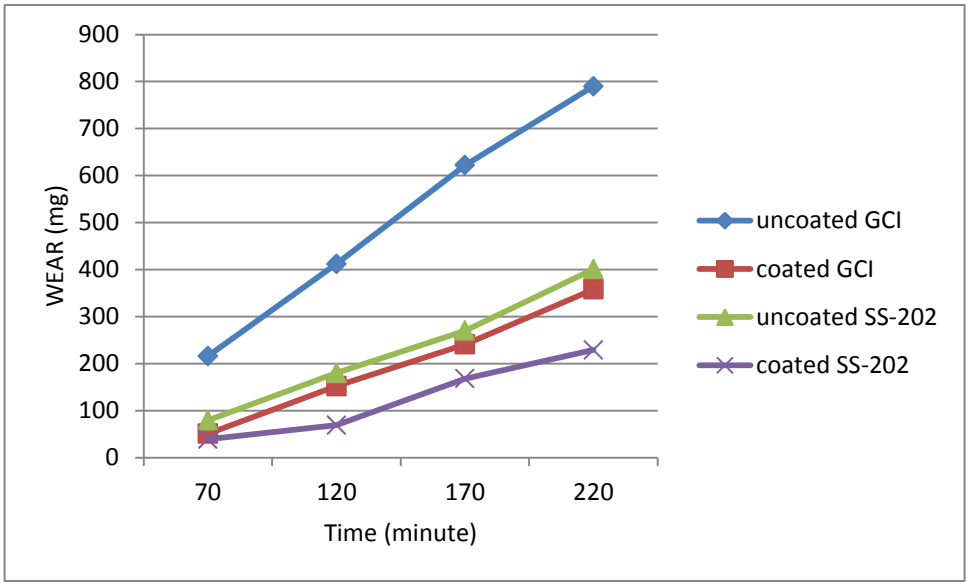

The above graph shows the variation of wear of uncoated and $Ni+Cr_2O_3$ coated specimens at 800rpm and 25% concentration. This also shows the same trend as in the case of $Ni+Al_2O_3$. As we examine from the graphs there is a huge difference in the wear of uncoated and coated samples.

4.3.11 Comparison of Erosion Wear of Uncoated Grey Cast Iron, SS-202 and $Ni+Cr_2O_3$ Coated Specimens At 25% Concentration and 1100rpm.

Figure 4.15 wear rate of uncoated and coating of Ni+Cr_2O_3 SS-202, Grey Cast Iron at 25% concentration and 1100rpm

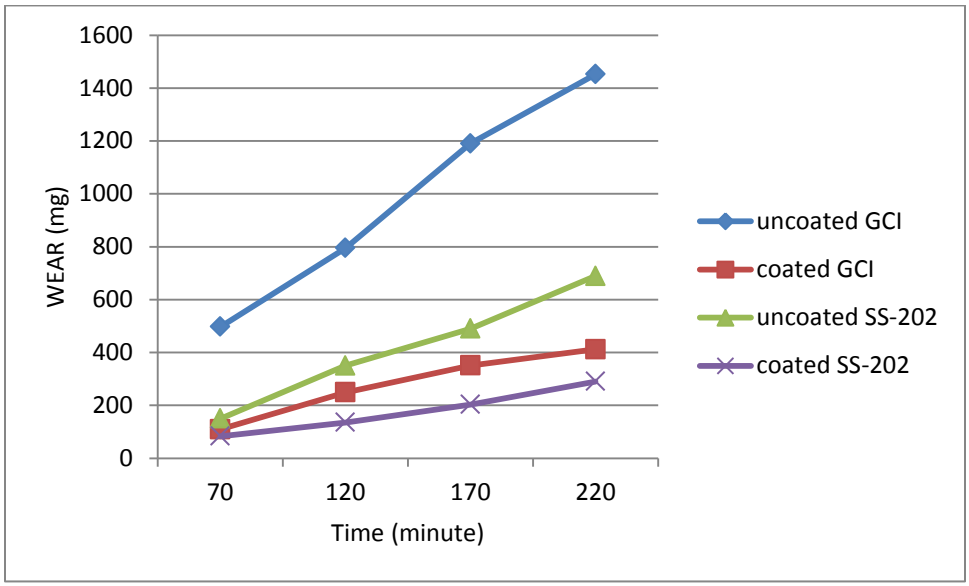

From figure 4.15 shows the variation of uncoated and Ni+Cr_2O_3 coated samples at 25% concentration and at 1100 minutes. The wear has increased as compared to the test conducted at 800rpm.

4.3.12 Comparison of Erosion Wear of Uncoated Grey Cast Iron, SS-202 and Ni+Cr_2O_3 Coated Specimens At 25% Concentration and 1400rpm.

Figure 4.16 wear rate of uncoated and coating of Ni+Cr_2O_3 SS-202, Grey Cast Iron at 25% concentration and 1400rpm

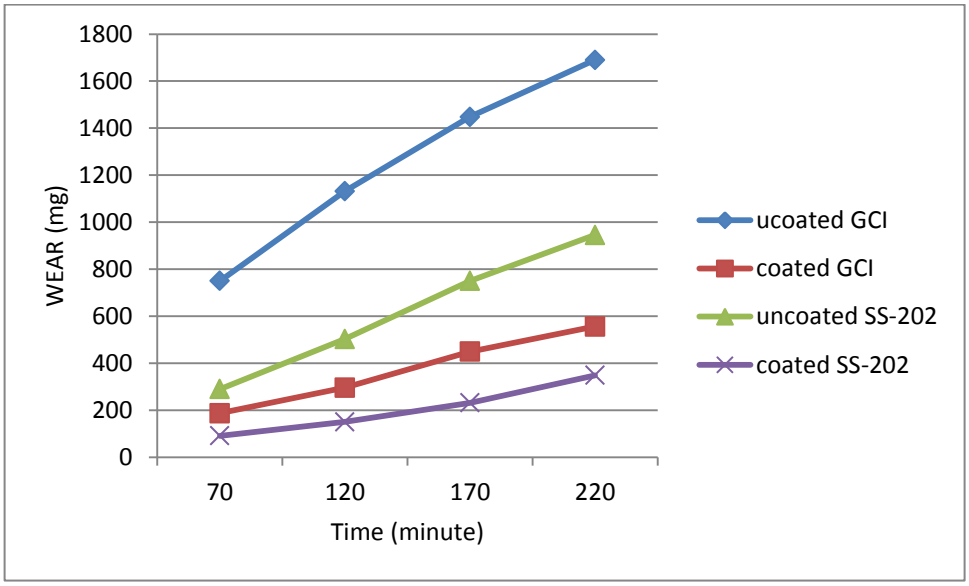

4.3.13 Comparison of Erosion Wear of Uncoated Grey Cast Iron, SS-202 and Ni+Al_2O_3 Coated Specimens At 45% Concentration and 800rpm.

Figure 4.17 wear rate of uncoated and coating of Ni+Al_2O_3 SS-202, Grey Cast Iron at 45% concentration and 800rpm

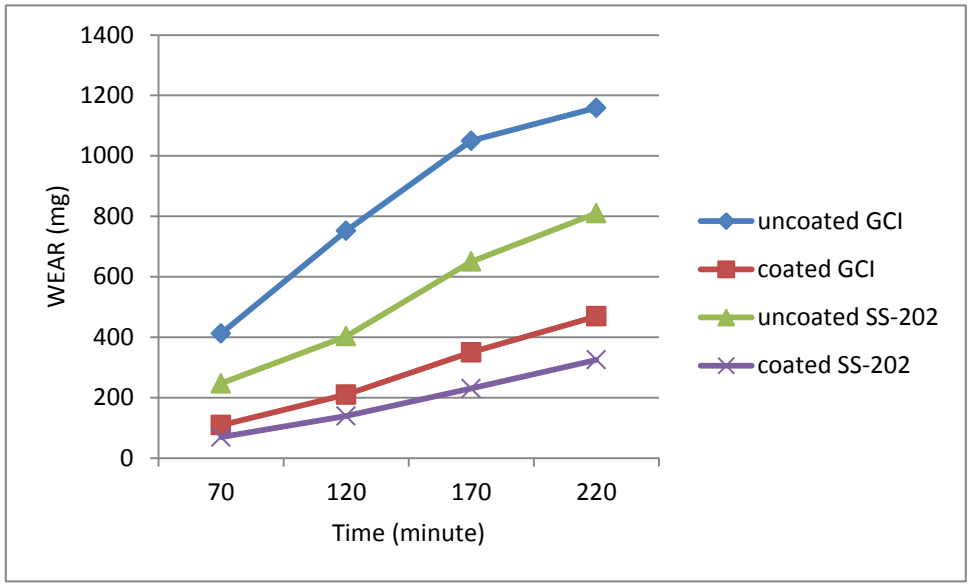

The above figure shows the erosion wear of uncoated and Ni+Al_2O_3 coated samples at 800rpm and 45% concentration. Now comparison of this graph with 25% concentration is that in this graph is more wear erosion occurred as a result wear is also dependent upon the concentration. Wear is proportional to the concentration of slurry. More is concentration of slurry more is erosion wear of specimen.

4.3.14 Comparison of Erosion Wear of Uncoated Grey Cast Iron, SS-202 and Ni+Al_2O_3 Coated Specimens At 45% Concentration and 1100rpm.

Figure 4.18 wear rate of uncoated and coating of $Ni+Al_2O_3$ SS-202, Grey Cast Iron at 45% concentration and 1100rpm

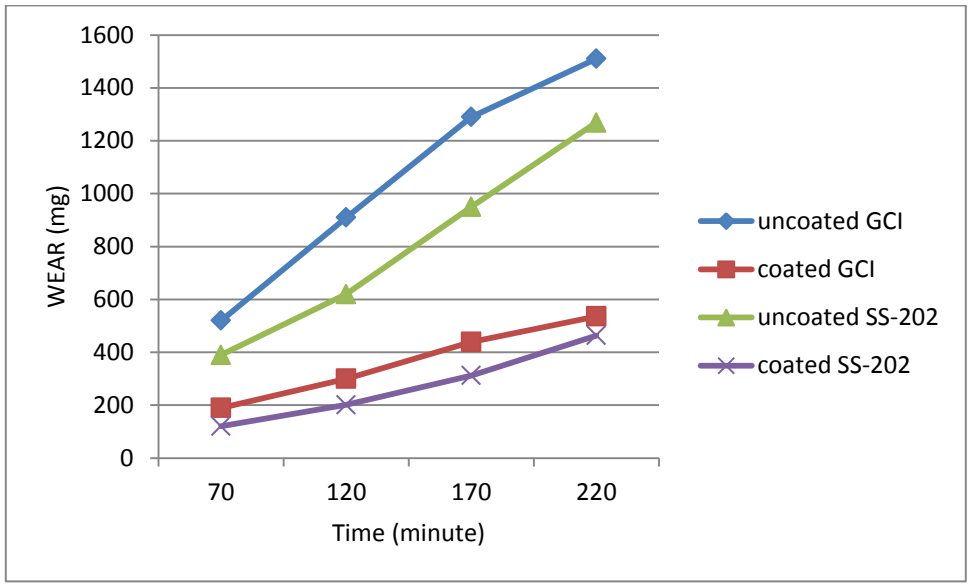

The above figure shows the comparison of wear loss in case of coated and uncoated samples at 1100rpm and 45% concentration of ash. Comparing it with figure 4.17, it can be observed that with increase in time the wear loss has increased.

4.3.15 Comparison of Erosion Wear of Uncoated Grey Cast Iron, SS-202 and $Ni+Al_2O_3$ Coated Specimens At 45% Concentration and 1400rpm.

Figure 4.19 wear rate of uncoated and coating of $Ni+Al_2O_3$ SS-202, Grey Cast Iron at 45% concentration and 1400rpm

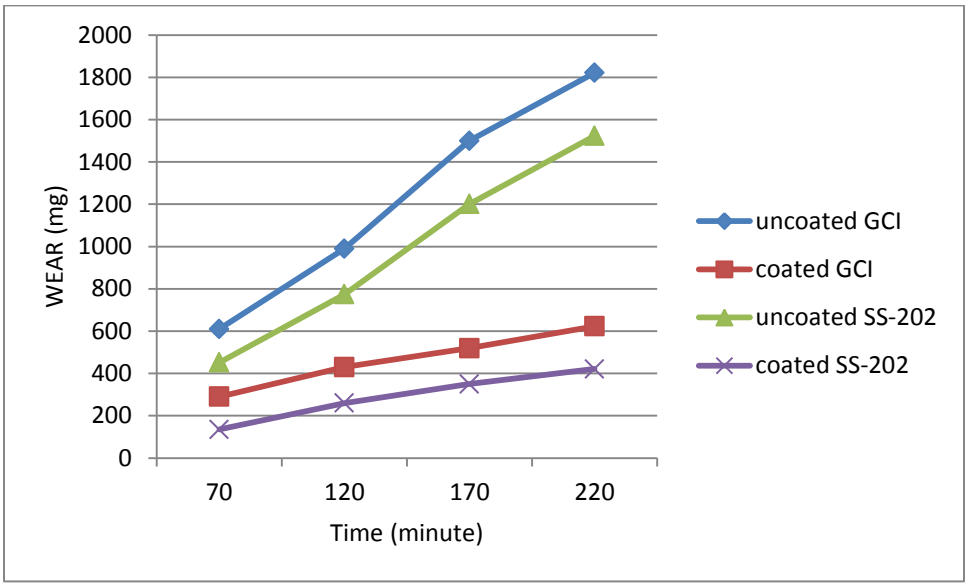

From the above 4.17, 4.18, 4.19 figures it can be examine that the loss of material due to wear increases with speed. But concentration is also the main factor which affects the material loss due to erosion. As the results at 45% were compared with the 25%, it was observed as difference in the wear loss being greater in case of 45% concentration.

4.3.16 Comparison of Erosion Wear of Uncoated Grey Cast Iron, SS-202 and $Ni+Cr_2O_3$ Coated Specimens At 45% Concentration and 800rpm.

Figure 4.20 wear rate of uncoated and coating of Ni+Cr_2O_3 SS-202, Grey Cast Iron at 45% concentration and 800rpm

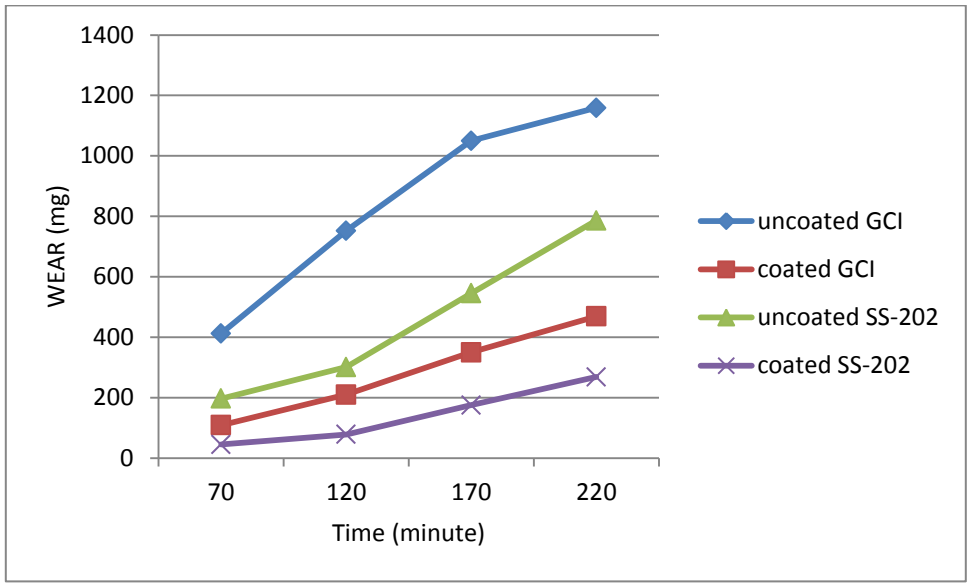

From above figure shows the results of the tests conducted at 45% concentration at 80 minutes with and without Ni+Cr_2O_3 coatings. It shows that the coating has decreased amount of wear. The wear increases with speed also in case of both coated and uncoated samples.

4.3.17 Comparison of Erosion Wear of Uncoated Grey Cast Iron, SS-202 and Ni+Cr_2O_3 Coated Specimens At 45% Concentration and 1100rpm.

Figure 4.21 wear rate of uncoated and coating of Ni+Cr_2O_3 SS-202, Grey Cast Iron at 45% concentration and 1100rpm

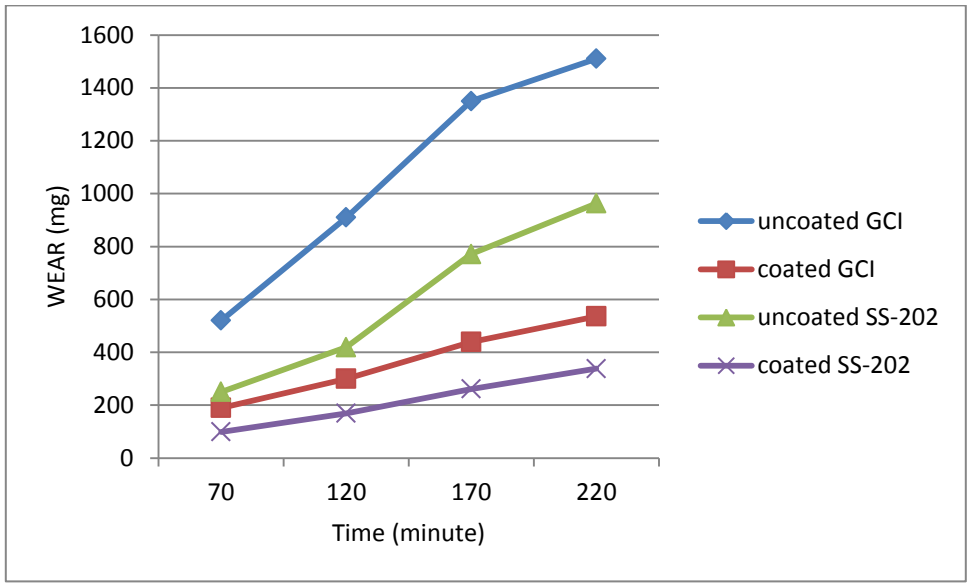

4.3.18 Comparison of Erosion Wear of Uncoated Grey Cast Iron, SS-202 and Ni+Cr_2O_3 Coated Specimens At 45% Concentration and 1400rpm.

Figure 4.22 wear rate of uncoated and coating of Ni+Cr_2O_3 SS-202, Grey Cast Iron at 45% concentration and 1400rpm

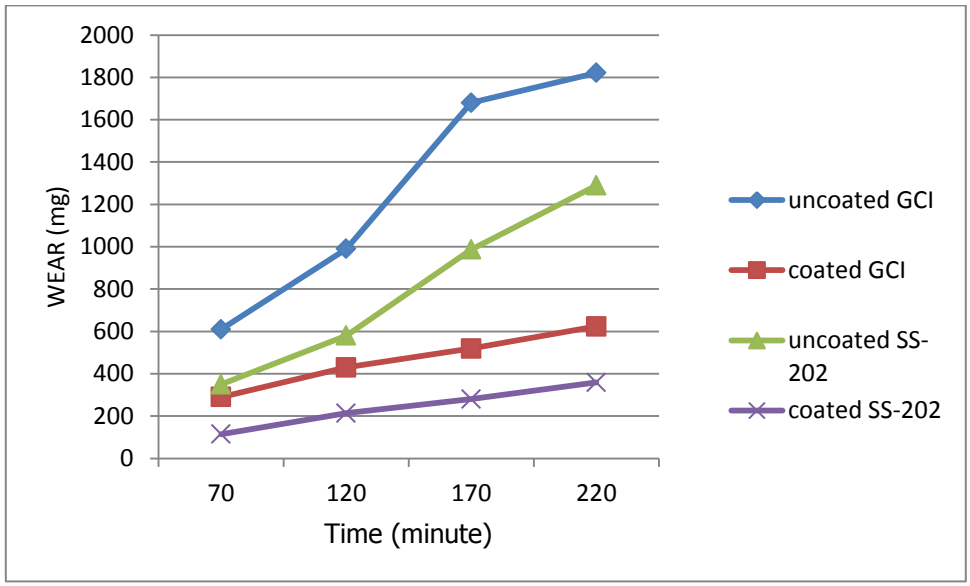

In the above figures 4.21 and 4.22 it can be seen that coating has marginally decreased the wear of the samples. In both graphs wear is dependent on the speed. As we discussed earlier wear is more if speed is more. Wear is proportional to the time, concentration.

4.4 SEM Analysis Of Erosion Affected Pieces

Analyses of samples were subjected to erosion at 45% concentration, 120 minutes and at 1400 rpm speed. Following are the images produced by SEM after the erosion wear.

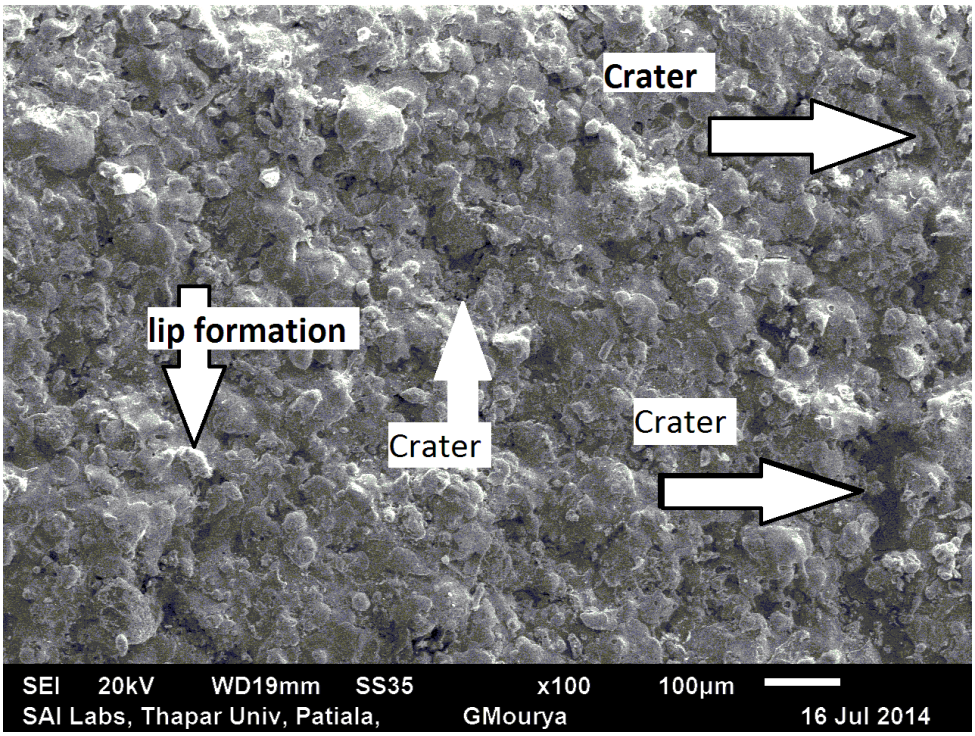

Figure 4.23 SEM analysis of Ni+Al_2O_3 coated Grey cast iron surface at X100

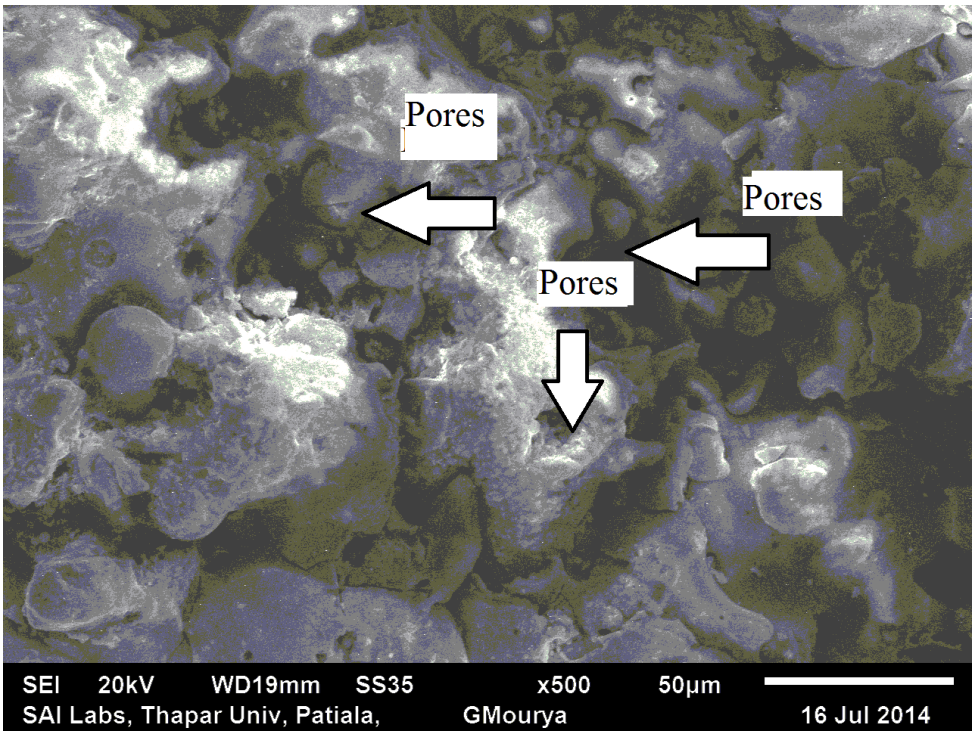

Figure 4.24 SEM analysis of Ni+Al_2O_3 coated Grey cast iron surface at X500

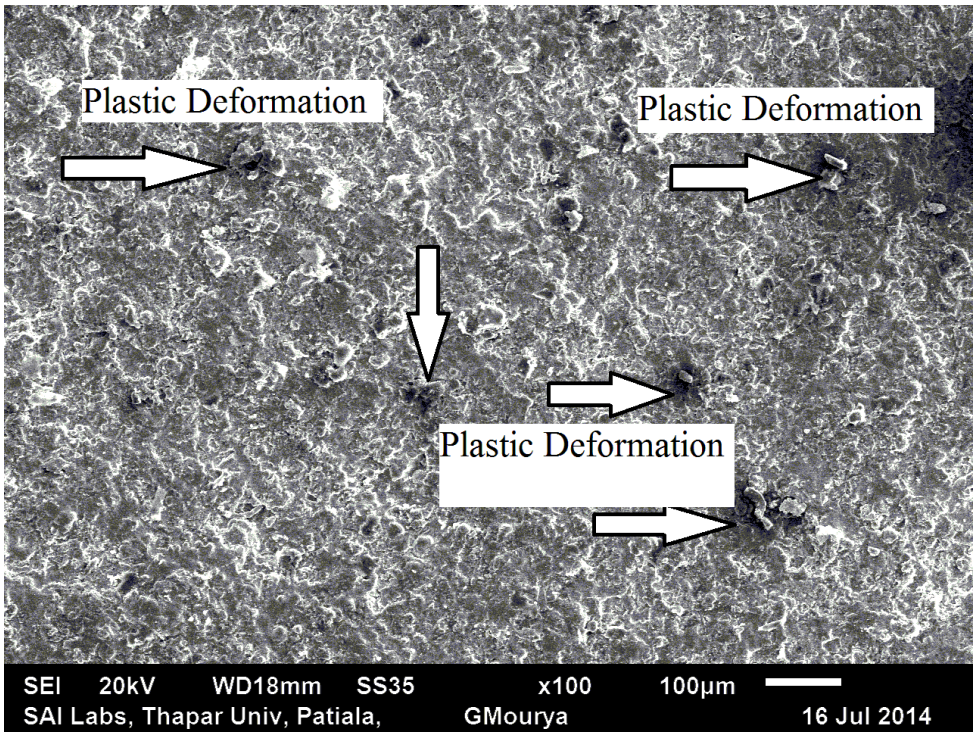

Figure 4.25 SEM analysis of Ni+Cr_2O_3 coated Grey cast iron surface at X100

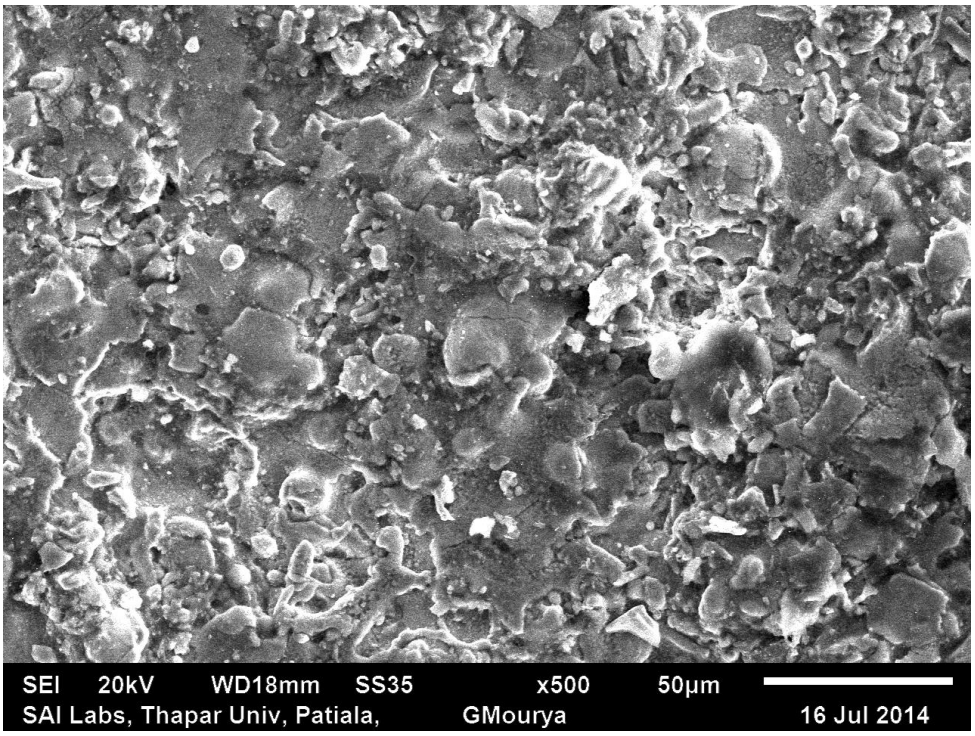

Figure 4.26 SEM analysis of Ni+Cr_2O_3 coated Grey cast iron surface at X500

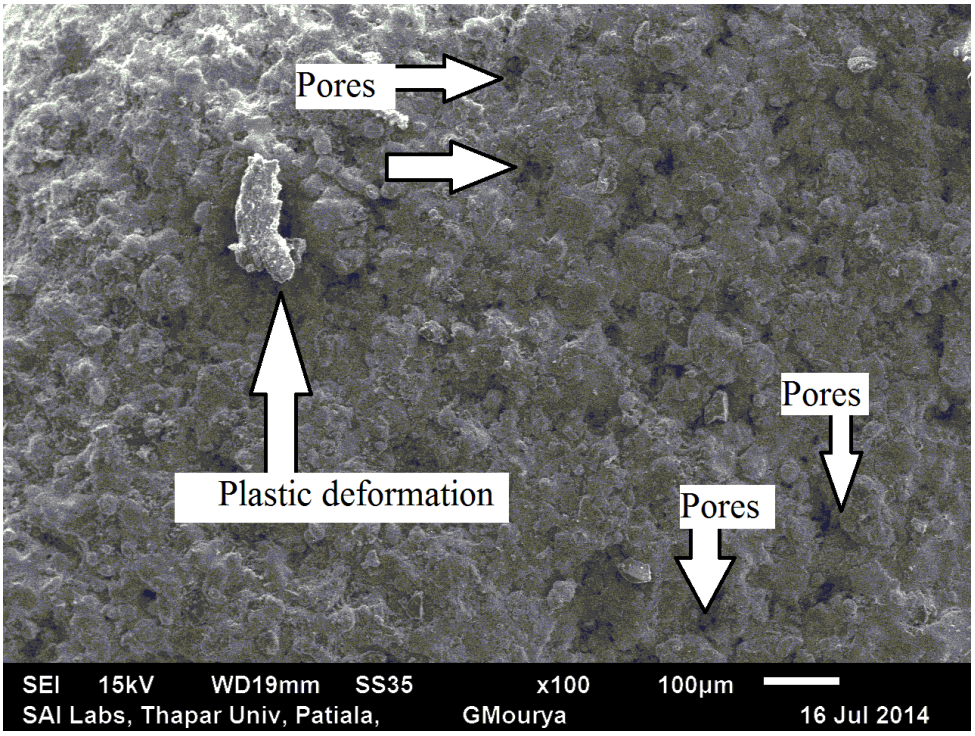

Figure 4.27 SEM analysis of Ni+Al_2O_3 coated of SS 202 surface at X100

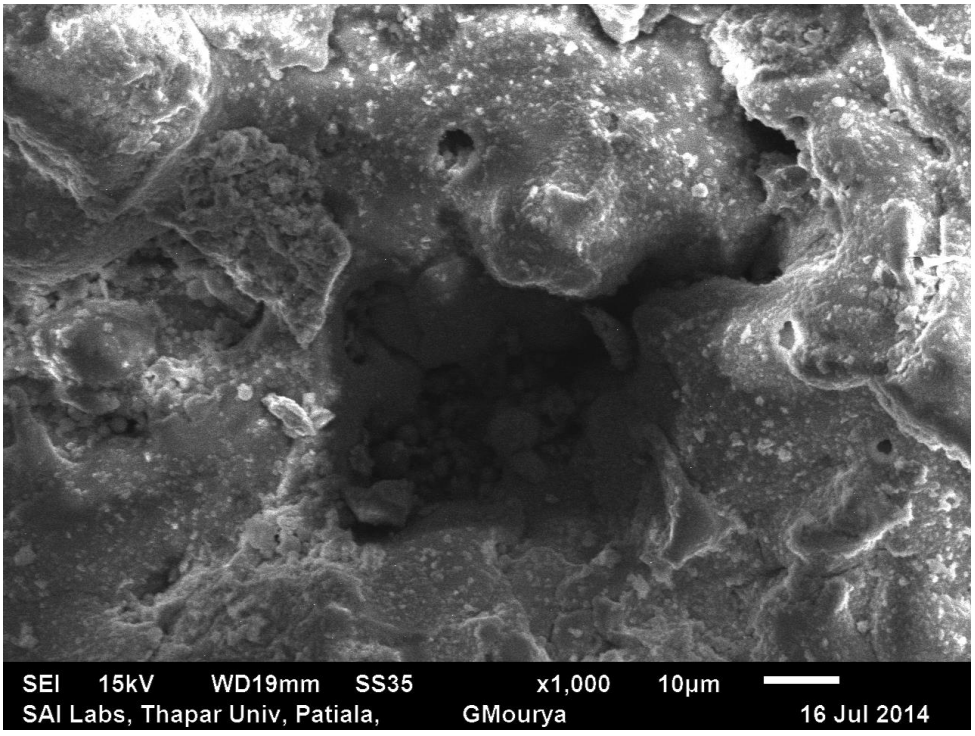

Figure 4.28 SEM analysis of Ni+Al_2O_3 coated of SS 202 surface at X1000

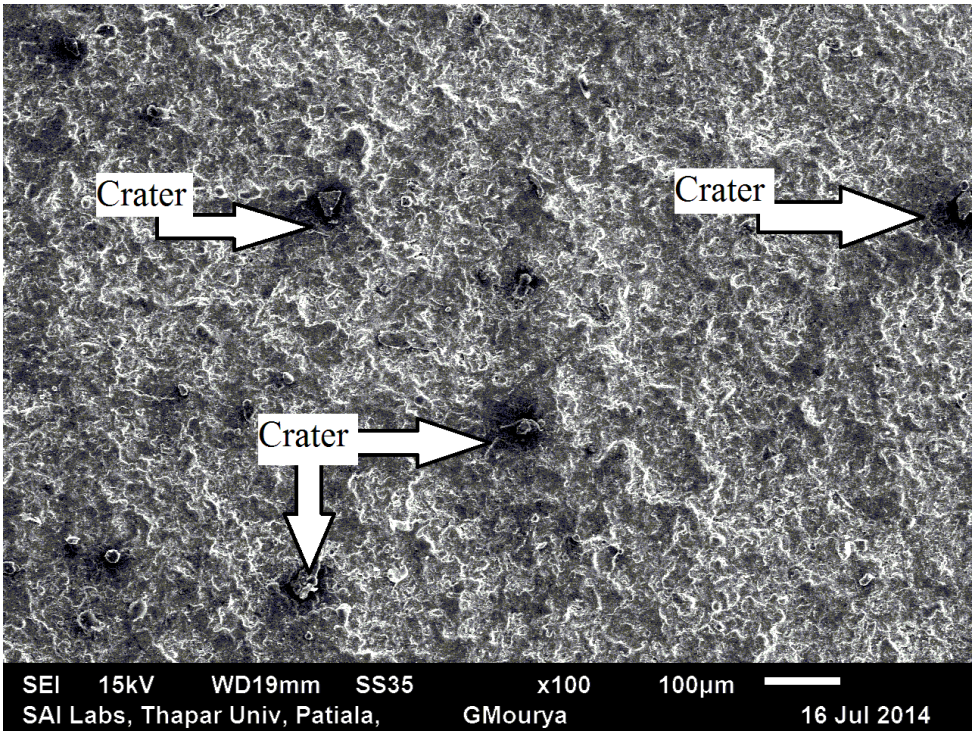

Figure 4.29 SEM analysis of Ni+Cr_2O_3 coated of SS 202 surface at X100

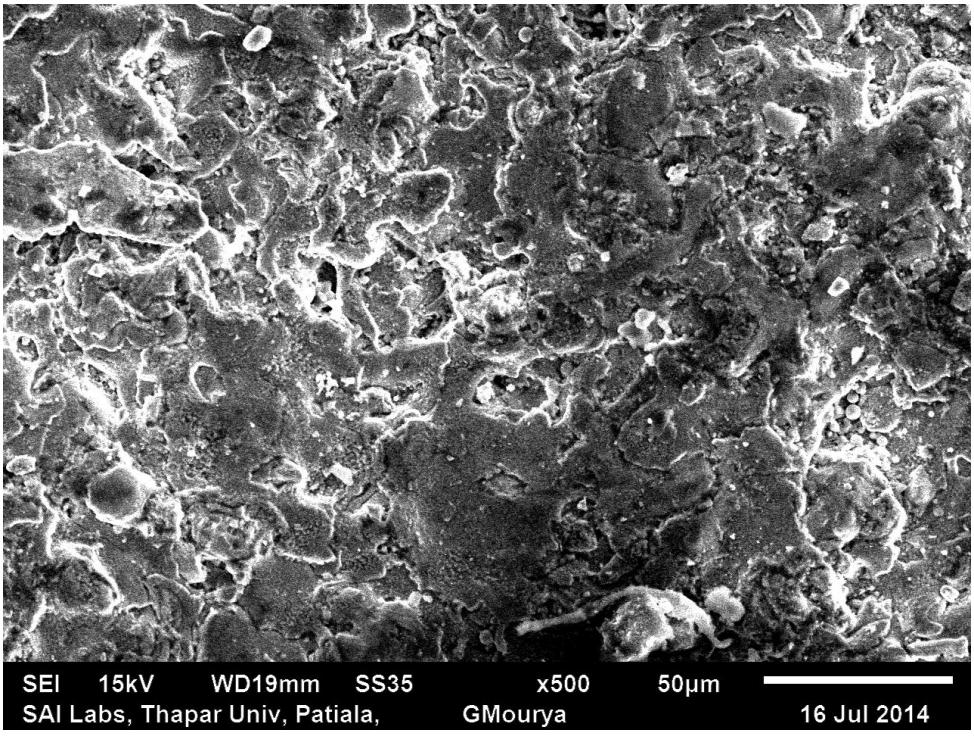

Figure 4.30 SEM analysis of Ni +Cr_2O_3 coated of SS 202 surface at X500

From above figures the images produced by SEM after erosion at 45% slurry, 120 minutes time and speed at 1400 rpm at magnification of X500, X100 and X1000. The pattern of erosion shows the formation of lips, pores, and craters in the above figure.

Chapter 5

Conclusions and Scope for Future Work

5.1 Conclusions

In all these investigations erosion wear under the effect of the parameters which affects the erosion wear of slurry pump materials. In this study we studied the erosion wear of with and without coating specimen. There are the comparison of erosion wear of coated and uncoated materials weight loss of both is determined. There is Ni+Al2O3, Ni+Cr2O3 coated and uncoated materials SS-202 and Grey cast iron are used to study erosion wear and fly ash slurry is taken as erodent medium, slurry pot tester is used to conduct the erosion tests. Speed exponent and slurry concentration exponent that are calculated in present experimental results are also compared with past research works. High velocity oxy-fuel process is used to deposit coatings on SS 202 and Grey cast iron materials.

- SS 202 shows better erosion resistance under all parameters as comparison of grey cast iron.
- Excellent improvement in hardness is reported in case of Ni+Cr2O3 coated materials as compared to Ni+Al2O3 coated materials.
- Erosion wear is dependent all parameters like speed, time, hardness, concentration of slurry.
- Ni+Cr2O3 coating shows improvement in erosion wear resistance of both materials as comparison of Ni+Al2O3.
- Speed exponent and concentration exponent values for all the materials are found in good agreement with previous research works.

5.2 Scope for Future Work

- The similar erosion wear studies can be extended by using other types of pot tester and different slurry concentration.
- The erosion wear studies can be performed with other coating techniques.

- The computational approach can be used to simulate the similar work with different operating conditions.
- The effect of erosion wear of pump impeller of ash disposal system can be studied.
- The friction wear studies can be performed on other type of testers at different parameters.

Chapter 6

References

[1] H.X. Zhao, H. Goto, M. Matsumura, T. Takahashi, M. Yamamoto, Slurry erosion of plasma-sprayed ceramic coatings, Surface and Coatings Technology 115, 1999, pp. 123–131.

[2] R.J. Llewellyn, S.K. Yick, K.F. Dolmanb, Scouring erosion resistance of metallic materials used in slurry pump service, Wear 256, 2004, pp. 592–599.

[3] M. Mehta, J.R. Cadamb, Velocity measurement of particle in the impeller of centrifugal slurry pump, Wear, 2004, pp. 241-249.

[4] T. Kumar, P. Jambulingam, M. Gopal and A. Rajadurai, Surface hardening of aisi 304, 316, 304l and 316l ss using cyanide free salt bath nitriding process, International Symposium of Research Students on Materials Science and Engineering Chennai, India, 2004, pp. 653-661.

[5] C.N. Machioa, G. Akdogana, M.J. Witcombb, S. Luyckxa(2005), Performance of WC–VC–Co thermal spray coatings in abrasion and slurry erosion tests, Wear 258, pp. 434–442.

[6] V.A.D. Souza, A. Neville, Corrosion and synergy in a WC Co Cr HVOF thermal spray coating—understanding their role in erosion–corrosion degradation, Wear 259, 2005, pp. 171–180.

[7] S. Shrestha, T. Hodgkiess, A. Neville , Erosion–corrosion behaviour of high-velocity oxy-fuel Ni–Cr–Mo–Si–B coatings under high-velocity seawater jet impingement, Wear 259, 2005, pp. 208–218.

[8] Kenichi Sugiyama, Shuhei Nakahamab, Shuji Hattoric, Keisuke Nakanoc , Slurry wear and cavitation erosion of thermal-sprayed cermets, Wear 258, 2005, pp. 768–775.

[9] K.S. Tan, J.A. Wharton, R.J.K. Wood, Solid particle erosion–corrosion behaviour of a novel HVOF nickel aluminium bronze coating for marine applications—correlation between mass loss and electrochemical measurements, Wear 258, 2005, pp. 629–640.

[10] Y. Iwai, T. Miyajima, T. Hondaa, T. Matsubara, K. Kandac, S. Hogmarkd, Evaluation of erosive wear resistance of TiN coatings by a slurry jet impact test, Wear 261, 2006, pp. 112–118.

[11] Sh. Khameneh Asl, M. Heydarzadeh Sohi, K. Hokamotoa, M. Uemurad, Effect of heat treatment on wear behavior of HVOF thermally sprayed WC-Co coatings, Wear 260, 2006, pp. 1203–1208.

[12] Y. Wang, Y. Yang, M.F. Yan, Microstructures, hardness and erosion behavior of thermal sprayed and heat treated NiAl coatings with different ceria, Wear 263, 2007, pp. 371–378.

[13] Khalid, Addie Graeme and Yu Wi-Chung, Effects of non-newtonian mineral suspensions on the performance of centrifugal pumps, Mineral Processing and Extractive Metallurgy Review, Vol20:1, 2007, pp. 239 – 249.

[14] Oka, Singh S. N., Seshadri V., Performance characteristics of centrifugal slurry pumps", Journal of Fluids Engineering ,Vol. 123, 2007, pp. 271-280.

[15] M.M. Stack, T.M. Abd El-Badia, Some comments on mapping the combined effects of slurry concentration, impact velocity and electrochemical potential on the erosion–corrosion of WC/Co–Cr coatings, Wear 264, 2008, pp. 826–837.

[16] V. Balasubramanian, R. Varahamoorthy, C.S. Ramachandran, S. Babu, Abrasive slurry wear behavior of stainless steel surface produced by plasma transferred arc hardfacing process", Journal of Surface & Coatings Technology 202, 2008, pp. 3903–3912.

[17] Girish R. Desalea, Bhupendra K. Gandhib, S.C. Jain(2009) , "Particle size effects on the slurry erosion of aluminium alloy (AA 6063)", Journal of Wear 266, pp 1066–1071

[18] J.F. Santa, L.A. Espitia, J.A. Blanco, S.A. Romo, A. Toro, Slurry and cavitation erosion resistance of thermal spray coatings, Wear 267, 2009, pp. 160–167.

[19] H.H. Tian, G.R. Addie, R.J. Visintain , Erosion–corrosion performance of high-Cr cast iron alloys in flowing liquid–solid slurries, Wear 267, 2009, pp. 2039–2047.

[20] K. Yıldızlı, M.B. Karamıs, F. Nair, Erosion mechanisms of nodular and gray cast irons at different impact angles, Wear 261, 2009, pp. 622–633.

[21] M.R. Ramesha, S. Prakashb, S.K. Nathb, Pawan Kumar Saprab, B. Venkataramanc, Solid particle erosion of HVOF sprayed WC-Co/NiCrFeSiB coatings, Wear 269, 2010, pp. 197–205.

[22] P. Purandare, A.P. Ehiasarian, M.M. Stack, P.Eh. Hovsepian, CrN/NbN coatings deposited by HIPIMS: A preliminary study of erosion–corrosion performance, Surface & Coatings Technology 204, 2010, pp. 1158–1162.

[23] R.J. Chunga, X. Tanga, D.Y. Li, B. Hinckleyb, K. Dolmanb, Abnormal erosion–slurry velocity relationship of high chromium cast iron with high carbon concentrations, Wear 271, 2011, pp. 1454– 1461.

[24] S.S. Rajahram, T.J.Harvey, R.J.K.Wood, Electrochemical investigation of erosion–corrosion using a slurry pot erosion tester, Tribology International 44, 2011, pp. 232–240.

[25] T.R. Umaa, J.B. Simhab, K. Narasimha Murthy, Influence of nickel on mechanical and slurry erosive wear behaviour of permanent moulded toughened austempered ductile iron, Wear 271, 2011, pp. 1378– 1384.

[26] B.W. Maurer, A.C. Gustafson, S.K. Bhatia, A.M. Palomino, Geotextile dewatering of flocculated, fiber reinforced fly-ash slurry, Fuel 97, 2012, pp. 411–417.

[27] H.S. Grewal, Anupam Agrawal, H. Singh, Slurry erosion performance of Ni–Al2O3 based composite coatings, Tribology International 66, 2013, pp. 296–306.

[28] Lalit Thakur, Navneet Arora, A comparative study on slurry and dry erosion behavior of HVOF sprayed WC–CoCr coatings, Wear303, 2013, pp. 405–411.

[29] E. Huttunen-Saarivirta, H. Kinnunen, J.Tuiremo, M. Uusitalo, M. Antonov, Erosive wear of boiler steels by sand and ash", Wear, 2014, pp. 1628-1635.

[30] Q.B. Nguyen, C.Y.H.Lim, V.B.Nguyen, Y.M.Wan, B.Nai, Y.W.Zhang , M.Gupta, Slurry erosion characteristics and erosion mechanisms of stainless steel, Journal of Tribology International 79, 2014, pp. 1–7.